

Comparison of different methods for calculating the paramagnetic relaxation enhancement of nuclear spins as a function of the magnetic field

Elie Belorizky, Pascal H. Fries, Lothar Helm, Jozef Kowalewski, Danuta Kruk, Robert R. Sharp, and Per-Olof Westlund

Citation: *The Journal of Chemical Physics* **128**, 052315 (2008); doi: 10.1063/1.2833957

View online: <http://dx.doi.org/10.1063/1.2833957>

View Table of Contents: <http://scitation.aip.org/content/aip/journal/jcp/128/5?ver=pdfcov>

Published by the [AIP Publishing](#)

Articles you may be interested in

[Characterizing longitudinal and transverse relaxation rates of ferrofluids in microtesla magnetic fields](#)
J. Appl. Phys. **110**, 123911 (2011); 10.1063/1.3671420

[Relaxation rates of protons in gadolinium chelates detected with a high- \$T_c\$ superconducting quantum interference device in microtesla magnetic fields](#)
J. Appl. Phys. **108**, 093904 (2010); 10.1063/1.3493737

[Structural defects in \$\text{LiCoO}_2\$ studied by \$^7\text{Li}\$ nuclear magnetic relaxation](#)
Appl. Phys. Lett. **96**, 062504 (2010); 10.1063/1.3310012

[General treatment of paramagnetic relaxation enhancement associated with translational diffusion](#)
J. Chem. Phys. **130**, 174104 (2009); 10.1063/1.3119635

[Nuclear magnetic resonance-paramagnetic relaxation enhancements: Influence of spatial quantization of the electron spin when the zero-field splitting energy is larger than the Zeeman energy](#)
J. Chem. Phys. **109**, 4035 (1998); 10.1063/1.477003



2014 Special Topics

PEROVSKITES

2D MATERIALS

MESOPOROUS MATERIALS

BIOMATERIALS/
BIOELECTRONICS

METAL-ORGANIC
FRAMEWORK
MATERIALS

AIP | APL Materials

Submit Today!

Comparison of different methods for calculating the paramagnetic relaxation enhancement of nuclear spins as a function of the magnetic field

Elie Belorizky,¹ Pascal H. Fries,² Lothar Helm,³ Jozef Kowalewski,^{4,a)} Danuta Kruk,⁵ Robert R. Sharp,⁶ and Per-Olof Westlund⁷

¹Laboratoire de Spectrométrie Physique, CNRS-UMR 5588, Université Joseph Fourier, BP 87, F-38402 Saint-Martin d'Hères Cédex, France

²Laboratoire de Reconnaissance Ionique et Chimie de Coordination, Service de Chimie Inorganique et Biologique (UMR-E 3 CEA-UJF), CEA/DSM/Département de Recherche Fondamentale sur la Matière Condensée, CEA-Grenoble, F-38054 Grenoble Cédex 9, France

³Ecole Polytechnique Fédérale de Lausanne, Laboratoire de Chimie Inorganique et Bioinorganique, EFPL-BCH, CH-1015 Lausanne, Switzerland

⁴Department of Physical, Inorganic and Structural Chemistry, Arrhenius Laboratory, Stockholm University, S-106 91 Stockholm, Sweden

⁵Institute of Physics, Jagiellonian University, Reymona 4, PL-30059 Krakow, Poland

⁶Department of Chemistry, University of Michigan, Ann Arbor, Michigan 48109, USA

⁷Department of Chemistry, Umeå University, S-90187 Umeå, Sweden

(Received 28 November 2007; accepted 18 December 2007; published online 1 February 2008)

The enhancement of the spin-lattice relaxation rate for nuclear spins in a ligand bound to a paramagnetic metal ion [known as the paramagnetic relaxation enhancement (PRE)] arises primarily through the dipole-dipole (DD) interaction between the nuclear spins and the electron spins. In solution, the DD interaction is modulated mostly by reorientation of the nuclear spin-electron spin axis and by electron spin relaxation. Calculations of the PRE are in general complicated, mainly because the electron spin interacts so strongly with the other degrees of freedom that its relaxation cannot be described by second-order perturbation theory or the Redfield theory. Three approaches to resolve this problem exist in the literature: The so-called slow-motion theory, originating from Swedish groups [Benetis *et al.*, *Mol. Phys.* **48**, 329 (1983); Kowalewski *et al.*, *Adv. Inorg. Chem.* **57**, (2005); Larsson *et al.*, *J. Chem. Phys.* **101**, 1116 (1994); T. Nilsson *et al.*, *J. Magn. Reson.* **154**, 269 (2002)] and two different methods based on simulations of the dynamics of electron spin in time domain, developed in Grenoble [Fries and Belorizky, *J. Chem. Phys.* **126**, 204503 (2007); Rast *et al.*, *ibid.* **115**, 7554 (2001)] and Ann Arbor [Abernathy and Sharp, *J. Chem. Phys.* **106**, 9032 (1997); Schaeffle and Sharp, *ibid.* **121**, 5387 (2004); Schaeffle and Sharp, *J. Magn. Reson.* **176**, 160 (2005)], respectively. In this paper, we report a numerical comparison of the three methods for a large variety of parameter sets, meant to correspond to large and small complexes of gadolinium(III) and of nickel(II). It is found that the agreement between the Swedish and the Grenoble approaches is very good for practically all parameter sets, while the predictions of the Ann Arbor model are similar in a number of the calculations but deviate significantly in others, reflecting in part differences in the treatment of electron spin relaxation. The origins of the discrepancies are discussed briefly. © 2008 American Institute of Physics.

[DOI: [10.1063/1.2833957](https://doi.org/10.1063/1.2833957)]

I. INTRODUCTION

Measurements of the enhancement of the solvent proton spin-lattice relaxation rate caused by paramagnetic ions or complexes are important sources of structural and dynamic information on the species present in solution. The enhancement is commonly called *paramagnetic relaxation enhancement* (PRE). At not too high concentration of the paramagnetic species, the PRE is proportional to the concentration. A common concept in the context is *relaxivity*, referring to the PRE normalized to 1 mM concentration of the paramagnetic

species. Measurements of the nuclear relaxation rate over a broad range of magnetic fields are referred to as *relaxometry*, and the resulting curve is denoted as a *nuclear magnetic relaxation dispersion* (NMRD) profile. The measurements and interpretation of the NMRD profiles in a variety of systems containing paramagnetic metal ions was the subject of Ref. 1.

On the experimental side, the NMRD profiles are usually measured by the field-cycling technique (where the magnetic field is rapidly switched between different values),^{1,2} by shuttling the sample between a high field of a superconducting magnet and a lower field outside,³ by measurements at several different “conventional” spectrometers, by a broadband spectrometer, or by a combination of the aforementioned

^{a)}Author to whom correspondence should be addressed. Electronic mail: jk@physc.su.se.

methods. The interpretation of the NMRD profiles amounts to formulating an appropriate model and fitting the parameters of the model to the experimental data. The theory of nuclear spin relaxation in paramagnetic systems with electron spins $S > 1/2$ is complicated for several reasons. First, we have the fact that the electronic spin motion is driven by two noncommuting Hamiltonians, namely, the time independent Zeeman Hamiltonian (H_{Zeem}) arising from the interaction of the electronic spin with the laboratory magnetic field and the zero-field splitting (ZFS) Hamiltonian (H_{ZFS}), which arises from the spin-orbit coupling for a $S \geq 1$ ion. The former Hamiltonian is diagonal in the laboratory coordinate frame ($z \parallel B_0$), the latter in the molecule-fixed ZFS principal axis system. The two Hamiltonians are generally of comparable magnitude for most d -block $S > 1/2$ ions, so that over the range of field strengths of a NMRD experiment, it is common to pass from the ZFS limit ($H_{ZFS} \gg H_{Zeem}$) at low field strengths to the Zeeman limit ($H_{Zeem} \gg H_{ZFS}$) at high fields. In passing through the intermediate regime of field strengths ($H_{ZFS} \approx H_{Zeem}$), the electron spin motion changes from a spatial quantization that is molecule fixed in the ZFS limit to a spatial quantization that is laboratory fixed in the Zeeman limit. Both the spin energy level structure and the zero-order spin wavefunctions change profoundly as a function of field strength as the system passes between the ZFS and Zeeman limits.

Further complicating the physical picture is the fact that H_{ZFS} is time dependent due to Brownian reorientation of the solute. Because of this motion, the electron spin eigenfunctions are stochastic functions of time. In the intermediate regime, the situation is particularly complex, since the spin wavefunctions are time-dependent quantities which lack distinct spatial quantization along either laboratory- or molecule-fixed axes. Still another source of complexity involves random distortions of the ZFS tensor due to thermal motions of the metal coordination sphere. ZFS distortion results both from intermolecular collisions and from thermal excitation/deexcitation of the normal vibrational modes of the metal coordination sphere. These processes are stochastic and provide mechanisms of electron spin relaxation. They play a fundamental role in the theory of the NMR-PRE.

One difficulty is caused by the fact that the electron spin relaxation is often beyond the validity range of the second-order perturbation treatment^{5,6} or the Redfield theory.⁷ For instance, this treatment is not applicable to the following frequent situation involving the mean ZFS interaction in the molecular frame bound to the complex, when the product of the interaction strength (in angular frequency units) and the characteristic time of the Brownian reorientation (the rotational correlation time τ_R) is not much smaller than unity and, simultaneously, τ_R is not long enough to justify that this interaction remains static in the laboratory frame, so that its effects can be calculated by a powder average over all the orientations of the complex. The three theoretical approaches described here are valid for the difficult case where molecular reorientation occurs at a similar rate as the coherent motions of the electron spin.

A further complication arises in the description of the dynamics of the process in which the ZFS tensor is distorted

during intermolecular collisions. The resulting stochastic ZFS tensor fluctuation provides a mechanism of electron spin relaxation, and in this way it influences the NMR-PRE. The selection of a dynamical model, which is both realistic and amenable to theoretical analysis and mathematical solution is a difficult problem that is discussed further below.

It is only in the Zeeman limit and in the perturbation regime that the physical picture of the relaxation phenomena is reasonable simple. It was for the purpose of describing this limiting case that the classical theory of the NMR-PRE was developed by Solomon, Bloembergen, and Morgan⁸⁻¹¹ (SBM) several decades ago. Since that time, advances in the theory have been formulated in laboratories in Sweden (S), Ann Arbor (AA), Grenoble (G), and Florence (F). The objective of this paper is to compare the results of these formulations with respect to the description of the effects of a time-dependent ZFS Hamiltonian. The outline is as follows. We present some of the current theoretical tools briefly in the theoretical section. The emphasis of this study is on actual numerical comparisons for two sets of parameters, presented in the results and discussion section. The first set has been chosen to represent systems of interest as gadolinium(III)-based contrast agents for magnetic resonance imaging.¹²⁻¹⁵ The second set corresponds to Ni(II) complexes. These systems are interesting mainly because of the challenge they represent for various theories. Some concluding remarks are presented in the final section of the paper.

II. THEORETICAL

A. Formulation of the problem

The magnetic dipole-dipole (DD) interaction has early been recognized as a source of nuclear spin relaxation. A very important early formulation of the problem of dipolar relaxation was presented in the classical paper of Bloembergen, Purcell, and Pound (BPP) from 1948,¹⁶ who indeed set the ground for all subsequent development. A few years later, Solomon considered a system of two nonequivalent spins I and S , both characterized by the spin quantum number of $1/2$, with the dipole-dipole interaction as the mechanism of spin relaxation.⁸ Through this work, some minor mistakes of the BPP formulation were corrected. Solomon and Bloembergen^{9,10} showed also that the scalar interaction between the I and S spins can act as a relaxation mechanism. For the cases under consideration in this work, paramagnetic enhancement of the spin-lattice relaxation, the dipole-dipole interaction is normally much more important and here we neglect the scalar contribution.

In order to cause relaxation, the dipole-dipole coupling has to be modulated by random processes. The next issue to consider are the processes generating this modulation. In a simple diamagnetic case, discussed for example in Abragam's book¹⁷ or in the recent book by Kowalewski and Mäler,¹⁸ we need to deal with two such dynamic processes: Reorientation of the spin-spin vector with respect to the laboratory frame and the mutual translational diffusion of the species carrying the I and S spins. In the PRE context, these two dynamic processes are associated with the so-called inner-sphere and outer-sphere relaxation enhancement. In

this study we treat only the inner-sphere case. In paramagnetic IS systems, where S denotes the electron spin, or sometimes in diamagnetic systems with a nuclear spin $I=1/2$ having a DD coupling to another nuclear spin $I' \geq 1$ with a quadrupolar moment,¹⁹ one needs, in addition, to consider the fact that the relaxation of the spins S and I' can modulate the DD interaction. This is a major complication in the PRE theory.

Thus, we consider the relaxation of a nuclear spin I in an external magnetic field B_0 , occurring due to the time fluctuations of the Hamiltonian, $H_{\text{dip}}(t)$, describing its magnetic dipole-dipole interaction with an electronic spin S . Let γ_I be the magnetogyric ratio of I and $\omega_I \equiv -\gamma_I B_0$ its angular Larmor frequency. The Hamiltonian of the nuclear (n) spin I is

$$H_n(t) = \hbar \omega_I I_z + H_{\text{dip}}(t). \quad (1)$$

It is convenient to express $H_{\text{dip}}(t)$ in the spherical tensor basis. Let μ_B be the Bohr magneton and g_S the Landé factor of S . The magnetic moments of the nuclear and electronic spins are $(m_I)_q^{(1)} = \gamma_I \hbar I_q^{(1)}$ and $(m_S)_q^{(1)} = -g_S \mu_B S_q^{(1)}$. Let (r_{IS}, θ, ϕ) be the spherical coordinates of the I - S interspin vector \mathbf{r}_{IS} in the laboratory (L) frame. The spherical harmonics $Y_{2q}(\theta, \phi)$ form a tensor of order 2, $\mathbf{Y}_2 \equiv (Y_{2q}(\theta, \phi))$ ($q = -2, \dots, 2$). The dipolar Hamiltonian $H_{\text{dip}}(t)$ describes the magnetic energy of the nuclear spin I in the local dipolar field of S , $(B_S)_q^{(1)}$ created by the electronic magnetic moment, i.e.,

$$H_{\text{dip}}(t) = -\mathbf{m}_I(t) \cdot \mathbf{B}_S(t) = -\gamma_I \hbar \sum_{q=-1}^{+1} (-)^q (B_S)_{-q}^{(1)}(t) (m_I)_q^{(1)}(t), \quad (2)$$

where $(B_S)_q^{(1)}$ is proportional to the rank-one part of the tensor product⁶ of \mathbf{Y}_2 and \mathbf{S} ,

$$\begin{aligned} (B_S)_q^{(1)} &= \frac{\mu_0}{4\pi} 2\sqrt{2\pi} g_S \mu_B \frac{1}{r_{IS}^3} (\mathbf{Y}_2 \otimes \mathbf{S})_q^{(1)} \\ &= \frac{\mu_0}{4\pi} 2\sqrt{6\pi} g_S \mu_B \sum_{m,m'} (-)^{1+q} \begin{pmatrix} 2 & 1 & 1 \\ m & m' & -q \end{pmatrix} \\ &\quad \times \frac{Y_{2m}(\theta, \phi)}{r_{IS}^3} S_{m'}^{(1)}. \end{aligned} \quad (3)$$

Paramagnetic NMR relaxation is driven by the resonant component of the dipolar interaction between the nuclear magnetic moment and the local dipolar field of S , \mathbf{B}_S . Specifically, the paramagnetic enhancement of the NMR spin-lattice relaxation rate $R_{1M} = T_{1M}^{-1}$ is proportional to the dipolar power density at the nuclear Larmor frequency ω_I . Because of the equality $(B_S)_{-1}^{(1)}(t)^\dagger = -(B_S)_1^{(1)}(t)$, it can be written as

$$T_{1M}^{-1} = -2\gamma_I^2 \text{Re} \int_0^\infty \overline{\langle (B_S)_{+1}^{(1)}(t) \cdot (B_S)_{-1}^{(1)}(0) \rangle} e^{-i\omega_I t} dt, \quad (4)$$

where the brackets indicate a quantum mechanical trace over the variables of S , and the superscripting line indicates a thermal average over the spatial molecular degrees of freedom.

Thus the evaluation of the time correlation functions (TCF) of the dipolar field,

$$\Gamma_{B,m} = -\overline{\langle (B_S)_m^{(1)}(t) \cdot (B_S)_{-m}^{(1)}(0) \rangle}, \quad (5)$$

forms the core of the problem. In part, the time dependence of $\mathbf{B}_S(t)$ arises from the fluctuations of the lattice functions $Y_{2m}(\theta, \phi)$ and r_{IS} in Eq. (3). For the inner-sphere case considered here, I and S belong to the same rigid molecule, r_{IS} is time independent, and $Y_{2m}(\theta, \phi)$ fluctuate due to Brownian reorientation.

Furthermore, the time dependence in $\mathbf{B}_S(t)$ arises from the electron spin motions as described by the spin TCF's

$$\Gamma_{S,m} = -\overline{\langle S_m^{(1)}(t) S_{-m}^{(1)}(0) \rangle}, \quad (6a)$$

$$= -\text{Tr} \{ \rho_S^\circ \overline{U_S(t) S_m^{(1)} U_S(t)^\dagger S_{-m}^{(1)}} \}, \quad (6b)$$

where $\rho_S^\circ = 1/(2S+1)$ is the high temperature thermal equilibrium density operator of S and $U_S(t)$ its time evolution operator. The motions of S are driven by the electron spin Hamiltonian H_S , which consists of a sum of two terms (neglecting the effects of nuclear hyperfine interactions): (1) The electronic Zeeman interaction (H_{Zeem}) and (2) the ZFS (H_{ZFS}),

$$H_S(\alpha, \beta, \gamma, t) = H_{\text{Zeem}} + H_{\text{ZFS}}(\alpha, \beta, \gamma; t). \quad (7)$$

The Zeeman and ZFS Hamiltonians do not in general commute; H_{Zeem} is diagonal in the L coordinate frame ($z \parallel B_0$), while $H_{\text{ZFS}}(\alpha, \beta, \gamma; t)$ is diagonal in the molecule-fixed ZFS principal axis system (P). Assuming that B_0 is constant, H_{Zeem} can be written as

$$H_{\text{Zeem}} = g_S \mu_B \mathbf{B}_0 \cdot \mathbf{S} = g_S \mu_B B_0 S_z = \hbar \omega_S S_z. \quad (8)$$

The ZFS term is diagonal in the P frame, which fluctuates in liquids due to Brownian reorientation. H_{ZFS} depends on even powers of the spin components and, written in the (P) frame, has the general form²⁰

$$\begin{aligned} H_{\text{ZFS}} &= D(S_z^2 - S(S+1)/3) + E(S_x^2 - S_y^2) + 4\text{th O.T.} \\ &\quad + 6\text{th O.T.} + \dots \end{aligned} \quad (9)$$

The individual terms on the right hand side of Eq. (9) may, in specific cases, vanish either by reason of the dimension of the spin space or because of chemical symmetry. For example, ZFS terms that are n th order in the spin operators are present for $n \leq 2S$ (n even). Hence for $S=1/2$, H_{ZFS} vanishes; for $S=1$ and $S=3/2$, only quadratic ZFS terms are present; for $S=2$ and $5/2$, quadratic and fourth order terms are present, etc. Chemical symmetry can further restrict the form of Eq. (9).

Equation (9) is written in the (P) frame, while the Zeeman and dipolar Hamiltonians [Eqs. (1)–(5)] are written in the (L) frame. Thus we transform Eq. (9) from (P) to (L) by first writing H_{ZFS} in the spherical basis²¹ in the (P) frame [denoted by superscripts ($\hat{\ }^{\prime}$)],

$$H_{\text{ZFS}} = \sqrt{2/3} D \hat{S}_0^{(2)} + E(\hat{S}_{+2}^{(2)} + \hat{S}_{-2}^{(2)}) + \text{h.o.t.}, \quad (10)$$

and then transforming the spin tensor operators from (P) to (L) using Wigner rotation matrices.⁶ For example,

$$\hat{S}_q^{(\ell)} = \sum_{q'} D_{q',q}^{(\ell)}(\alpha, \beta, \gamma) S_{q'}^{(\ell)}, \quad (11)$$

where (α, β, γ) are the Euler angles defining the orientation of (P) with respect to (L) . Details of the calculation are given elsewhere.⁶ In liquids, the P frame (and hence H_{ZFS}) is time dependent due to Brownian reorientation. Thus H_S and H_{ZFS} are written in Eq. (7) as functions of both molecular orientation and of time.

It is usual to separate $H_{ZFS}(\alpha, \beta, \gamma, t)$ into a pair of terms describing, respectively, the “permanent” (or “static”) and “collisional” (or “transient”) ZFS interactions,

$$H_{ZFS}(\alpha, \beta, \gamma, t) = H_{ZFS,S}(\alpha, \beta, \gamma, t) + H_{ZFS,T}(t). \quad (12)$$

The permanent ZFS interaction, $H_{ZFS,S}(\alpha, \beta, \gamma, t)$, is time independent in the P frame; this quantity is the value of $H_{ZFS}(\alpha, \beta, \gamma, t)$ after averaging over vibrations and other molecular internal degrees of freedom, as well as over distortions of the ZFS tensor caused by intermolecular collisions. Thus $H_{ZFS,S}(\alpha, \beta, \gamma, t)$ is permanent in the sense of a permanent electric dipole moment. The collisional term, $H_{ZFS,T}(t)$, results from thermal modulation of the ZFS tensor by processes other than Brownian reorientation. Such processes include collisionally induced distortions of the ZFS tensor and thermal modulation due to vibrational relaxation. $H_{ZFS,T}(t)$ fluctuates with zero mean on the time scale of a few picoseconds and often provides a mechanism of electron spin relaxation. The decomposition into the static and transient ZFS is most useful if the time scales of rotations (on the one hand) and other motions (on the other hand) are significantly different.

The effect on the electronic spin motions of $H_{ZFS,S}(\alpha, \beta, \gamma, t)$ is more complex than that of $H_{ZFS,T}(t)$ in that it depends on the rate of molecular reorientation and on the value of B_0 . At sufficiently low field, when reorientation is slow compared to the inverse transition frequencies, $H_{ZFS,S}(\alpha, \beta, \gamma, t)$ can be considered stationary, in which case this term drives coherent oscillations of the matrix elements of S . When molecular reorientation is fast, $H_{ZFS,S}(\alpha, \beta, \gamma, t)$ induces stochastic motions in $\langle S \rangle$ and thus provides a second mechanism of electron spin relaxation in addition to that due to $H_{ZFS,T}(t)$. It is therefore, useful to distinguish “fast” and “slow” regimes of molecular reorientation with respect to the role of $H_{ZFS,S}(\alpha, \beta, \gamma, t)$ in the theory. The intermediate regime where the spin oscillations of $H_{ZFS,S}(\alpha, \beta, \gamma, t)$ and molecular reorientation occur on the same time scale is naturally more difficult to treat than are the limiting cases.

B. Early theoretical models

An early theory of the PRE phenomenon was given in the form of modified Solomon-Bloembergen (MSB) equations, first presented by Connick and Fiat²² and by Reuben *et al.*²³ and formally derived by Gueron²⁴ and Benetis *et al.*²⁵ The dipolar part of the MSB equations can be written as

$$T_{1M}^{-1} = \frac{2}{15} S(S+1) C_{DD}^2 \left[\frac{\tau_{c2}}{1 + (\omega_S - \omega_I)^2 \tau_{c2}^2} + \frac{3\tau_{c1}}{1 + \omega_I^2 \tau_{c1}^2} + \frac{6\tau_{c2}}{1 + (\omega_S + \omega_I)^2 \tau_{c2}^2} \right]. \quad (13)$$

Here, $C_{DD} \equiv (\mu_0/4\pi) \gamma_I \gamma_S \hbar / r_{IS}^3$ denotes the dipole-dipole coupling constant with $\gamma_S \hbar = -g_S \mu_B$, and the other symbols have their usual meaning. The correlation times τ_{ci} are defined as

$$\tau_{ci}^{-1} \equiv \tau_R^{-1} + T_{ie}^{-1} + \tau_M^{-1}, \quad i = 1, 2. \quad (14)$$

The symbol τ_R is the same as introduced above and represents the rank-two rotational correlation time. The MSB equations also allow for the chemical exchange of the I -spin-carrying ligand between the first coordination sphere of the transition metal and the bulk, characterized by the exchange lifetime τ_M . We neglect the chemical exchange as a modulation mechanism in this study. T_{1e} is the electron spin-lattice relaxation time and T_{2e} is the corresponding spin-spin relaxation time.

A simple theory of electron spin relaxation for $S \geq 1$ metal ions in aqueous solution was already formulated in the early sixties by Bloembergen and Morgan.¹¹ They considered the theory of the electron spin Hamiltonian dominated by the Zeeman interaction (the high field limit) and the static ZFS vanishing because of high (average) symmetry of the hydrated metal ions [$H_{ZFS,S}(\alpha, \beta, \gamma, t) = 0$]. The transient ZFS was assumed to have its origin in collisions of the hydrated ion with the surrounding solvent molecules, to be limited to the quadratic terms in Eq. (9) and to undergo rapid fluctuations. Using the second order perturbation theory and simplifying the problem a bit, they obtained that the longitudinal and transverse electron spin relaxation processes were simple exponential with the field-dependence of relaxation times according to

$$T_{1e}^{-1} = \frac{1}{5} \tau_{S0}^{-1} \left[\frac{1}{1 + \tau_v^2 \omega_S^2} + \frac{4}{1 + 4\tau_v^2 \omega_S^2} \right], \quad (15)$$

$$T_{2e}^{-1} = \frac{1}{10} \tau_{S0}^{-1} \left[3 + \frac{5}{1 + \tau_v^2 \omega_S^2} + \frac{2}{1 + 4\tau_v^2 \omega_S^2} \right], \quad (16)$$

where τ_v is the distortional or vibrational (ν) correlation time and τ_{S0} denotes the electron spin relaxation time at the limit $\tau_v^2 \omega_S^2 \ll 1$, where $T_{1e} = T_{2e}$.

The modified Solomon-Bloembergen equations can be combined with the Bloembergen-Morgan expressions for the electron spin relaxation rates, yielding a self-contained theory known as the SBM theory. The SBM theory has been extensively used over the years, in spite of the problems with its validity range.^{1,4} As discussed in a recent review,²⁶ the main limitations of the SBM theory are threefold. First, it is based on the assumption that the electron spin relaxation and the molecular reorientation are uncorrelated. This *decomposition approximation* is the essence of Eq. (14) and becomes problematic if the ZFS interaction has a nonvanishing average value in the molecular frame, which is modulated by the complex reorientation. Second, the unperturbed stationary Hamiltonian of the electron spin system is chosen to be the

Zeeman interaction, which corresponds to the high-field or Zeeman limit treatment of Eq. (7). Third, other interactions, such as the ZFS, are included by means of time-dependent second-order perturbation theory (the Redfield theory), yielding simple exponential relaxation processes characterized by a longitudinal and a transverse relaxation time. This set of assumptions can be violated in many ways: (1) At low magnetic field, the ZFS interaction can dominate over Zeeman [in fact the “low field” condition holds at all attainable laboratory magnetic field strengths for a number of important transition ions, e.g., high-spin Co(II) (Ref. 27)]; (2) the ZFS interaction may be too strong for the perturbation approach; and (3) even if the Zeeman and Redfield limits apply, the electron spin relaxation in high-spin systems ($S > 1$) is expected to be multiexponential. Besides these main assumptions, the SBM theory contains several other approximations, such as the point-dipole approximation and the assumptions that both the electronic g tensor and the reorientational motion are isotropic.⁴

In the Zeeman limit, the issue of the multiexponentiality of the electron spin relaxation can be resolved fairly easily, as discussed by Hudson and Luckhurst,²⁸ Rubinstein *et al.*,²⁹ and Westlund and Strandberg.^{30,31} There are also ways around the high-field limit assumption, at least under condition of very slow rotation of the complex.^{32–37} The problems with the decomposition approximation and with the Redfield limit are very fundamental and difficult to circumvent.

C. Assumptions and parameters

There are three approaches in the literature which claim to have solved these problems in rather different ways, and we have undertaken this study in order to obtain numerical comparisons of the NMRD profiles predicted by the three methods for some typical parameter sets. The assumptions of the three approaches differ, but there is a certain basic and common set that we follow.

(1) *The ZFS Hamiltonian.* The systems under consideration are characterized by $S \geq 1$ and a nonvanishing permanent (averaged over fast motions) quadratic ZFS. We assume that it is cylindrically symmetric in the molecular frame, i.e., two of its principal elements are equal. Combined with the traceless nature of the ZFS, this leads to a single parameter description of the mean ZFS, called the permanent or static ZFS and denoted by $\Delta_S \equiv \sqrt{2/3}D_S$. The spin Hamiltonian for the static ZFS is written as

$$H_{\text{ZFS},S}^{(P_S)} = D_S[S_z^2 - S(S+1)/3]. \quad (17)$$

The superscript (P_S) indicates explicitly that the Hamiltonian is formulated in the principal frame of the static ZFS, fixed in the molecule. In addition to the permanent value, the ZFS is characterized by spread, called transient (or “collisionally modulated”) ZFS and denoted by $\Delta_T \equiv \sqrt{2/3}D_T$. The corresponding Hamiltonian is expressed as

$$H_{\text{ZFS},T}^{(P_T)} = D_T[S_z^2 - S(S+1)/3]. \quad (18)$$

The superscript (P_T) means that the transient ZFS Hamiltonian is formulated in its own principal frame, which does

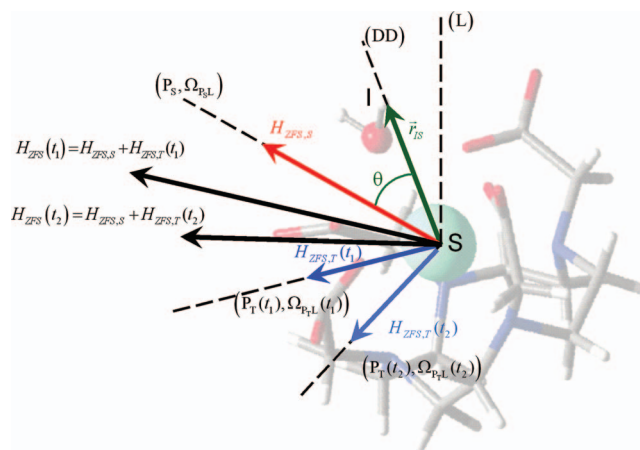


FIG. 1. (Color) Orientations of the principal axis systems for the static ZFS interaction (P_S) and the transient ZFS interaction (P_T) with respect to the laboratory frame (L) for a given orientation of the molecule. The red arrow represents the static ZFS, the blue arrows indicate the transient ZFS at two different times t_1 and t_2 , and the black arrows show the combined ZFS Hamiltonian H_{ZFS} at these times; the interspin vector \mathbf{r}_{IS} linking the electronic spin S and the nuclear spin I is shown in green together with the polar angle θ .

not coincide with the P_S frame. These concepts are illustrated in Fig. 1.

(2) *Reorientational dynamics.* There are two relevant dynamic processes. First, the molecular frame changes its orientation in the laboratory frame by means of isotropic rotational diffusion in small steps. The nature of this process is rather obvious and its role was discussed already in the BPP paper. For the motion of this kind, the time-correlation function of the rank-two spherical harmonics decays exponentially with a time constant called *rotational correlation time* τ_R , the quantity occurring in Eq. (14). The complex reorientation modulates the intramolecular (intracomplex) dipole-dipole interaction as well as the static ZFS interaction. The former modulation is a source of dipole-dipole relaxation, while the latter can yield electron spin relaxation.

(3) *Collisional dynamics.* The second dynamic process involves distortions of the complex caused by collisions with the surrounding solvent molecules and is more complicated. Rubinstein *et al.*²⁹ proposed a description of the process by a rotational diffusion equation and called it “pseudorotation.” The characteristic time constant for this motion is called *distortional correlation time* or pseudorotation correlation time. It can be identified with the parameter τ_ν in the Bloembergen-Morgan expressions [Eqs. (15) and (16)]. The pseudorotation time describes the reorientation of the transient ZFS of a constant magnitude Δ_T with respect to an arbitrary molecule fixed frame. In a system with vanishing static ZFS, the zero-field limit electron spin-relaxation time of the Bloembergen-Morgan expressions can be related to Δ_T and τ_ν ,

$$\tau_{S0}^{-1} = \frac{1}{5}[4S(S+1) - 3]\Delta_T^2\tau_\nu. \quad (19)$$

In a system where Δ_S is nonzero, τ_ν has a similar meaning, i.e., the correlation time for the part of the ZFS, which is averaged out on a time scale shorter than rotation. In the interpretation of Larsson *et al.*,³⁸ the intracomplex motion

described by τ_ν is called anisotropic pseudorotation, indicating that it affects the spread of the ZFS and leads to a non-zero mean. In the terminology of the group of Grenoble,^{20,39} this second dynamic process is simply referred to as *transient fluctuation*. It should be stressed that the ZFS distortional motions that are parametrized by the quantities Δ_T and τ_ν are in reality very complex. The pseudorotation model treats the collisional ZFS distortion as a classical diffusion over the surface of a sphere by a transient ZFS tensor of constant amplitude. The ZFS motions resulting from intermolecular collisions are physically rather different from this picture, however, in that a random sequence of molecular collisions produces a sequence of ZFS fluctuations with random amplitude and random orientation. The motion is intrinsically large step rather than diffusive in character. Thus the physical significance of the parameters (Δ_T and τ_ν) of the model is not entirely clear. Furthermore, in any real system the motion is complicated by the presence of several inequivalent degrees of freedom of the metal coordination sphere, and these degrees of freedom in general possess distinct compliance constants (i.e., there are several values of Δ_T and τ_ν). At present, the only analysis which takes these complexities into consideration in a realistic way is that of Odellius *et al.*,^{40,41} who analyzed collisional ZFS distortions in the $S=1$ Ni(II) hexaquaquation using a combination of MD simulation and *ab initio* quantum calculation. The present calculations employ motional models that are highly simplified compared to the more detailed analysis of these studies.

The Ann Arbor approach does not use the pseudorotation model to describe collisional dynamics, but rather the Redfield theory of Ref. 42. In its most general form, this theory calculates a set of eigenstate-specific electron spin relaxation rates in a manner which accounts (at least formally) for the five distortional modes of a quadratic ZFS tensor. The simplified form of the theory⁴³ used in this study averages the calculation over spin eigenstates and with respect to the modes of ZFS distortion. Thus the level of theoretical description parallels that of Bloembergen-Morgan theory with respect to the complexity of the physical parametrization and the calculated results (i.e., a single set of parameters, Δ_T and τ_ν , is used to calculate two eigenstate-averaged relaxation rates, $\tau_{S_1}^{-1}$ and $\tau_{S_2}^{-1}$, along the z and x laboratory axes), but it generalizes the Bloembergen-Morgan theory by incorporating the effects of the permanent ZFS Hamiltonian. Since this theory (like Bloembergen-Morgan theory) invokes the Redfield assumption ($\Delta_T\tau_\nu < 1$), it fails when Δ_T is large (see further below).

(4) *Orientation of the nuclear spin in the molecular frame.* The orientation of the permanent ZFS principal axis does not need to coincide with the dipole-dipole principal axis. Thus the polar angle θ between the interspin vector \mathbf{r}_{IS} and the ZFS principal axis may be different from zero. The calculations assume limiting values of $\theta=0$ and $\pi/2$.

These five parameters, Δ_R , Δ_T , τ_R , τ_ν , and θ , are used by all the three models to be compared with each other. Besides these quantities, the inner-sphere, dipole-dipole relaxivity at a given magnetic field depends on the dipole-dipole coupling constant (which in turn depends on the electron g_S factor, the magnetogyric ratio of the nuclear spin and the distance be-

tween the spins) and the chemical exchange lifetime τ_M . The chemical exchange lifetime is, throughout this study, assumed infinite (no exchange). The dipole-dipole coupling constant acts as a scaling factor.

D. The Swedish slow motion theory (the S method)

The approach developed by the Swedish groups^{25,26,38,44} uses the concept of a nuclear spin interacting with a composite lattice, containing the quantized electron spin degrees of freedom as well as classical molecular degrees of freedom. The composite lattice of this kind can be dealt with using a formulation based on the Liouville superoperators. The coupling between the nuclear spin and the lattice is through the dipole-dipole interaction between the nuclear and the electron spin (a scalar term can also be included, if required). The formulation of the dipole-dipole Hamiltonian is analogous to Eqs. (2) and (3),

$$H_{IL}^{DD} = \sum_{n=-1}^1 (-)^n I_n^{(1)} T_{-n}^{(1)}. \quad (20)$$

The operators I_n^1 are simply nuclear spin operators in irreducible spherical form, while the lattice operators T_{-n}^1 are rank-one contractions of the electron spin operators (rank-one) and the rank-two Wigner rotation matrices.^{25,26} The PRE is obtained by taking the real part of a complex spectral density function at the nuclear Larmor frequency,

$$\begin{aligned} T_{1M}^{-1} &= 2 \operatorname{Re} K_{1,1}^{DD}(-\omega_I) \\ &= 2 \operatorname{Re} \int_0^\infty \operatorname{Tr}_L \{ T_1^{(1)+} \exp(-i\hat{L}_L\tau) T_1^{(1)} \sigma^T \} \\ &\quad \times \exp(-i\omega_I\tau) d\tau. \end{aligned} \quad (21)$$

The expression under the integral sign, $\operatorname{Tr}_L \{ T_1^{(1)+} \exp(-i\hat{L}_L\tau) T_1^{(1)} \sigma^T \}$, is a time-correlation function for the lattice operators; σ^T is the equilibrium density operator for the lattice (subject to high-temperature approximation) and \hat{L}_L is the Liouville superoperator (Liouvillian) describing the lattice. Equation (21) is essentially identical to Eq. (4). Under the set of common assumptions described above, the lattice Liouville superoperator is a sum of “quantum” terms for the electron Zeeman and the ZFS (static and transient) interactions and classical Markov operators for the rotation of the complex as well as the pseudorotation. The calculations according to Eq. (21) are carried out using expansion of the lattice operators in a basis set, constructed as a direct product of Wigner rotation matrices (in two sets of Euler angles, corresponding to the rotational and distortional motions) and appropriate spin (super) operators. It should be stressed that the electron spin dynamics is never separated from the classical motions; thus, Eqs. (6) are never used. The nuclear spin-lattice relaxation rate, caused by the interaction with the electron spin (the PRE), is given by

$$\begin{aligned} T_{1M}^{-1} &= \frac{4}{3} (C_{DD})^2 S(S+1) \operatorname{Re} \{ \mathbf{c}_1^* [i(\mathbf{L}_L + \omega_I \mathbf{1})]^{-1} \mathbf{c}_1 \} \\ &= \frac{4}{3} (C_{DD})^2 S(S+1) \operatorname{Re} \{ \mathbf{c}_1^* \mathbf{M}^{-1} \mathbf{c}_1 \}, \end{aligned} \quad (22)$$

where \mathbf{L}_L is the matrix representation of the lattice Liouvil-

lean obtained using the basis set mentioned above and \mathbf{c}_1 is a projection vector representing the lattice operators in the same basis. The projection vector reduces greatly the number of elements of the $\mathbf{M}^{-1}=[i(\mathbf{L}_L+\omega_I\mathbf{1})]^{-1}$ matrix needed. The vector contains only three nonzero elements and a 3×3 fragment of the inverted matrix is required. Numerically, the calculations imply setting up a (very large) matrix and finding a fragment of the inverse matrix. Typically, the basis set size will be determined by the prespecified electron spin quantum number S and the L quantum numbers of the Wigner rotation matrices included in the basis set. In practice, the L quantum numbers are increased step by step, until convergence is reached. The matrix inversion is carried out using the Lanczos algorithm.

It should be mentioned that Åman and Westlund have reformulated the S theory in time domain.^{45,46} That time domain formulation is made in the Liouville space. For a simple example,⁴⁵ it has been shown that the S theory as presented above (called the Fokker-Planck approach by Åman and Westlund) gives results that are identical to this time domain method, called the Langevin approach. One could mention the advantage with a time domain approach, namely, that it is more flexible towards different dynamic models. The eigenfunction expansion of the diffusion propagator is in the time-domain approach replaced by calculation of trajectories.

E. The Grenoble approach (the G method)

The Grenoble approach starts with Eqs. (1)–(3). The time fluctuations of $H_{\text{dip}}(t)$ are due to both the random displacements of the interspin vector \mathbf{r}_{IS} and the random dynamics of the electronic spin states caused by the rotational and vibrational/collisional motion of the metal complex.^{21,47} The effects of the time fluctuations of $H_{\text{dip}}(t)$ on the nuclear relaxation are handled in a statistical way as follows. Consider a large number $N_{\text{sys}}\cong 2000\text{--}50\,000$ of random realizations j of the I - S spin system. Each realization j consists in a spatial trajectory $\mathbf{r}_{IS,j}(t)\equiv(r_{IS,jt},\theta_{jt},\phi_{jt})$ of the interspin vector and in rotational and vibrational trajectories of the metal complex inducing random fluctuations of the Hamiltonian $H_{1j}^{(L)}(t)$ acting on the electronic spin S and expressed in the L frame. The total Hamiltonian of the electronic spin of the realization j is

$$H_{e,j}^{(L)}(t) = H_{e0} + H_{1j}^{(L)}(t), \quad (23)$$

where $H_{e0}\equiv\omega_S S_z$ is the time-independent Zeeman Hamiltonian of the electronic spin. The operator $U_{ej}(t)$ giving the evolution of the electronic spin states of the realization j is the solution of the Schrödinger equation,⁶

$$idU_{ej}/dt = H_{e,j}^{(L)}(t)U_{ej} \quad \text{with } U_{ej}(0) = \mathbf{1}. \quad (24)$$

We introduce the time-dependent electronic spin component operators,

$$S_{jd}(t) \equiv U_{ej}(t)^\dagger S_{jd} U_{ej}(t) \quad (d=z, +, -). \quad (25)$$

The TCF of the component $(B_S)_{-1}^{(1)}$ of the local dipolar field \mathbf{B}_S is defined as

$$k_{-1}(t) = -\Gamma_{B,1}(t) \equiv \frac{1}{N_{\text{sys}}} \sum_{j=1}^{N_{\text{sys}}} \frac{1}{2S+1} \times \text{Tr}_S\{[(B_S)_{-1,j}^{(1)}(t)]^\dagger (B_S)_{-1,j}^{(1)}(0)\}, \quad (26)$$

where, according to Eq. (3) and using the abbreviation $\hat{r}_{jt} \equiv (\theta_{jt}, \phi_{jt})$, $(B_S)_{-1,j}^{(1)}(t)$ is

$$(B_S)_{-1,j}^{(1)}(t) = \frac{\mu_0}{4\pi} \sqrt{\frac{12\pi}{5}} g_S \mu_B \left[\frac{Y_{2,-2}(\hat{r}_{jt})}{r_{IS,jt}^3} S_{j+}(t) + \frac{Y_{2,-1}(\hat{r}_{jt})}{r_{IS,jt}^3} S_{jz}(t) - \frac{\sqrt{6} Y_{2,0}(\hat{r}_{jt})}{6 r_{IS,jt}^3} S_{j-}(t) \right]. \quad (27)$$

The longitudinal PRE, T_{1M}^{-1} , i.e., the increase of longitudinal relaxation rate of the nuclear spin I due to the electronic spins S , is given by

$$T_{1M}^{-1} = 2\gamma_I^2 \text{Re} \int_0^\infty k_{-1}(t) \exp(-i\omega_I t) dt. \quad (28)$$

As stated above, we are concerned with a perturbing Hamiltonian in the laboratory frame, $H_{1j}^{(L)}(t)$, arising from the time modulation of both the static and transient ZFS Hamiltonians. For the realization j of the spin system, let R_{jt} and R_{jt}^{ps} be the actual and pseudorotation which, at time t , transform the (L) frame into the molecular (P_S) and (P_T) frames, respectively. In the (L) frame, the total ZFS Hamiltonian is given by

$$H_{1j}^{(L)}(t) = H_{\text{ZFS},j}^{(L)}(t) = \Delta_S \sum_{q=-2}^2 D_{q0}^{(2)}(R_{jt}) S_q^{(2)} + \Delta_T \sum_{q=-2}^2 D_{q0}^{(2)}(R_{jt}^{\text{ps}}) S_q^{(2)}, \quad (29)$$

where the operators $S_q^{(2)}$ are the components of an irreducible tensor of order 2 and are called T_2^q in Refs. 20 and 21.

The practical evaluation of Eq. (28) is detailed in the Appendix. For an arbitrary field value, the above expression is computed by the trapezoidal rule, Eq. (A4), applied over a finite time interval $[0, t_{\text{max}}]$ with n_t equally spaced integration points separated by the time step Δt . At high field B_0 , i.e., for $\omega_S \gg \Delta_S$ and $\omega_S \gg \Delta_T$, $k_{-1}(t)$ tends to the real analytical approximation,

$$k_{-1}^{\text{high field}}(t) = \frac{3}{10} k_{-1}(0) \exp(-t/\tau_R) \exp(-t/T_{1e}), \quad (30)$$

where the longitudinal electronic relaxation is just given by the Bloembergen and Morgan equations [(15) and (19)], and is also named McLachlan expression in Ref. 21. This simplification results from the relative weights of the terms entering the expression [in Eq. (26)] of the TCF, $k_{-1}(t)$, of the local dipolar field component, $(B_S)_{-1,j}^{(1)}(t)$, given by Eq. (27). Indeed, as B_0 increases, the phase factors of the operators $S_{j\pm}(t)$ of $(B_S)_{-1,j}^{(1)}(t)$ have faster and faster oscillations which average out their contributions to $k_{-1}(t)$. The only remaining term involves the product $S_{jz}(t)S_{jz}(0)$, the ‘‘longitudinal’’ TCF which is still given at sufficiently high field by the standard Redfield relaxation theory,²¹ even beyond its expected validity range. This decay is due to the fluctuations of

the static and transient ZFS Hamiltonians, which according to the Redfield theory have high-field contributions to the decay rate proportional to $1/(\omega_S^2\tau_R)$ and $1/(\omega_S^2\tau_\nu)$, respectively. Since we have $\tau_\nu \ll \tau_R$, the high-field decay rate is driven by the transient ZFS, so that the decomposition approximation applies. Finally, the decay of the longitudinal TCF is monoexponential with a rate $1/T_{1e}$ defined above by the Bloembergen and Morgan expression, which is valid for $S=1$, but also for $S=7/2$.^{48,49} These properties are illustrated in Fig. 10 in the Appendix.

According to Eq. (29), it is shown in the Appendix that the high-field PRE can be approximated by the analytical expression

$$(T_{1M}^{-1})^{\text{high field}} \cong \left(\frac{\mu_0}{4\pi}\right)^2 \frac{2}{5} \gamma_I^2 g_S^2 \mu_B^2 S(S+1) \frac{1}{r_{IS}^6} \frac{\tau_{c1}}{1 + \omega_I^2 \tau_{c1}^2}, \quad (31)$$

where the correlation time τ_{c1} has the definition $1/\tau_{c1} \equiv 1/\tau_R + 1/T_{1e}$ corresponding to Eq. (14) with $\tau_M = \infty$. In Sec. III, it will be shown that at 23.5 T the high-field PRE values given by Eq. (31) agree to within a few percent with the Swedish results in the case of $S=1$ for ZFS parameters up to 10 cm^{-1} . In the case of the Gd(III) complexes with $S=7/2$, if $B_0 \geq 0.705 \text{ T}$, the same accuracy is reached for $\Delta_S, \Delta_T \leq 0.05 \text{ cm}^{-1}$.

It should be pointed out that the high-field expression, Eq. (31), is simply the contribution of the central term in $\omega_I \tau_{c1}$ of the modified SB approximation, Eq. (13), of the PRE. Even if the two terms in ω_S are dominant in the SBM theory, they have to be dropped. Indeed, when the metal complex is tumbling slowly ($\Delta_S \tau_R > 1$), the Redfield approximation should not be applied and leads to an unphysically too large T_{2e}^{-1} value roughly proportional to $\Delta_S^2 \tau_R$ and consequently to a too short value of τ_{c2} given by Eq. (14). Then, in Eq. (13), $\omega_S \tau_{c2}$ is too small, so that the terms in ω_S are too large. The same difficulty occurs in the case of a multiexponential mathematical solution of the Redfield equations.^{20,29–31,36} More precisely, when the metal complex is tumbling slowly, the transverse electronic relaxation times T_{2e} have particularly short unphysical values. Then, the transverse correlation time τ_{c2} given by Eq. (14) is also too short and $\omega_S \tau_{c2}$ is too small, so that the terms in ω_S of Eq. (13) are unphysically large. The system $S=7/2$, $\Delta_S = 0.01 \text{ cm}^{-1}$, $\Delta_T = 0.05 \text{ cm}^{-1}$, $\theta = 0$ or 90° , $\tau_R = 1 \text{ } \mu\text{s}$, $\tau_\nu = 5 \text{ ps}$ provides a typical example of the failure of Eq. (13) at high field. At 23.5 T, Eq. (13) gives a PRE value twice as large as that derived from Eq. (31).

We are now in a position to apply Eqs. (28) and (31) to calculate the paramagnetic relaxation enhancement, PRE $= T_{1M}^{-1}$, as a function of magnetic field for various sets of amplitudes Δ_S and Δ_T of the ZFS Hamiltonian, rotational correlation time τ_R of its static contribution and pseudorotational correlation time τ_ν of its transient contribution, modeling the vibrations/collisions of the complex. In the present work, restricted to intramolecular dipolar relaxation, the interspin vector \mathbf{r}_{IS} is fixed in the molecular (P_S) frame. The two situations, where \mathbf{r}_{IS} is parallel and perpendicular to the static ZFS symmetry axis $O\hat{z}$, will be studied. In the present

simulation, the stochastic dependence between the rotation of $\mathbf{r}_{IS,j}(t)$ and the evolution operator $U_{ej}(t)$ of the electronic spins states, which both depend on the same actual Brownian rotation of the metal complex, is fully taken into account. The so-called decomposition approximation,²⁶ which neglects this dependence to simplify the analytical approach, is avoided.

F. The Ann Arbor approach (the AA method)

The Ann Arbor theory, which was developed during the 1990s, describes the motion of the electron spin system in wavefunction space rather than Liouville space.^{33,34,50–52} In the present study, the time dependence of the problem is evaluated by means of spin dynamic (SD) simulation methods.^{53–55}

The Ann Arbor approach consists of a suite of algorithms which are implemented in the computer program PARELAX2.⁵⁵ Two of the algorithms are based on the “constant H_S ” approximation, which evaluates Eqs. (4)–(6) in either the (L) frame or the (P) frame under the assumption that the $H_{ZFS,S}(\alpha, \beta, \gamma; t)$ in Eq. (12) is constant in time. The theory is physically transparent when the problem is formulated in the coordinate frame corresponding to the spatial quantization of the electron spin motion. Thus, the P frame provides a natural description when the spin motion is in the vicinity of the ZFS limit and the L frame in the vicinity of the Zeeman limit. When the formulation is implemented in the natural frame, it is relatively straightforward to discern the effects and contributions of specific spin matrix elements and specific ZFS tensor components to the NMR-PRE. Thus, the constant H_S approach is especially useful for understanding the physics of the relaxation mechanism. It also provides a suitable platform for a more sophisticated description of collisional electron spin relaxation (see the discussion below). The principal limitation is that constant H_S ignores the reorientational mechanism of electron spin relaxation, i.e., relaxation resulting from the Brownian motion of $H_{ZFS,S}(\alpha, \beta, \gamma; t)$.

The third set of algorithms in PARELAX2, called spin dynamic (SD) simulation provides a more general computational platform which evaluates the TCFs of Eqs. (4)–(6) driven by the general spin Hamiltonian of Eq. (7).⁵⁴ This approach was used in this study. The SD algorithms are similar in spirit to molecular dynamics simulation: The molecular degrees of freedom are simulated as a classical random walk trajectory through the space of molecular orientations (i.e., the space of the Euler angles), while the electron spin degrees of freedom are propagated quantum mechanically. The reorientational model follows the ideas of Ivanov,⁵⁶ which assume that (1) molecular reorientation results from a sequence of rotational jumps which occur at randomly spaced intervals; (2) individual reorientational jumps are sudden, that is, they are rapid compared to the inverse transition frequencies of the spin system; (3) the rotation axes of individual jumps are oriented randomly in space; and (4) the magnitude of the jump angle is distributed as a Gaussian deviate of width σ_ϕ and zero mean.

The electron spin is propagated quantum mechanically

using a propagator calculated from the Hamiltonian, $H_S^\circ(\alpha, \beta, \gamma; t) = H_{Zem} + H_{ZFS,S}(\alpha, \beta, \gamma; t)$. This quantity is time independent in the intervals between jumps and changes suddenly during jumps. The spin propagator can be decomposed as follows:

$$U(t, t_0) = U^{(n)}(t, t_n) \cdots U'(t_2) U^{(1)}(t_2, t_1) U'(t_1) U^{(0)}(t_1, t_0), \quad (32)$$

where $U^{(n)}(t, t_n)$ is the propagator in the interval $t_n \rightarrow t_{n+1}$, and $U'(t_n)$ is the propagator for the jump at time t_n . If the jumps are rapid on the time scale of the spin oscillations driven by $H_S^\circ(\alpha, \beta, \gamma, t_n)$, the state vector is unaffected by the jump (this is the ‘‘Sudden Approximation’’ discussed in Chapter XVII of Ref. 6):

$$U'(t_n) = \underline{1}. \quad (33)$$

At the beginning of the n th interval, the spin Hamiltonian, $H_S^\circ(\alpha, \beta, \gamma, t_n)$, is computed, and the propagator $U^{(n)}(t, t_n)$ is evaluated from the series definition of the exponential operator. Then the spin TCF is evaluated at a sequence of time steps within the interval until the next jump occurs, when new values of $H_S^\circ(\alpha, \beta, \gamma, t_{n+1})$ and $U^{(n+1)}(t, t_{n+1})$ are evaluated. SD simulations evaluate $\Gamma_{B,m}(t)$ in Eq. (5) as an ensemble average of, typically, 5000 trajectories constructed in this way. The algorithms are stable and accurate over $>10^4$ time steps when the elementary time steps are small and when the spin propagation is carried out in double precision.

The treatment of the electron spin relaxation in the AA approach is an important issue, since it differs from the S and G methods. As described above, electron spin relaxation for $S \geq 1$ in the presence of a permanent ZFS interaction is usually attributed to two motional processes, namely, (1) reorientation of the permanent ZFS tensor and (2) collisional modulation of the permanent ZFS tensor as described by the stochastic Hamiltonian, $H_{ZFS,T}(t)$, in Eq. (12). Spin decay due to the reorientational process is calculated directly by the SD algorithms. The collisional contribution is evaluated separately using the theory of Refs. 42 and 43. The resulting decay functions, $\exp(-t/\tau_{S1})$ and $\exp(-t/\tau_{S2})$, are then applied to the spin TCFs of Eq. (6b).

The molecular dynamics of the collisional process are in general quite complex. There are, in the simplest case of uniaxial P -frame symmetry (as assumed in the calculations of this study), two distinct modes of ZFS distortion, axial and equatorial, which are described, in general, by different values Δ_T and τ_i ; that is, the force constants and thermal amplitudes of these motions differ. An example is provided by a planar metalloporphyrin, in which the compliance constants associated with in-plane displacements of the nitrogen atoms of the porphyrin moiety are much smaller (i.e., the bonding is tighter) than those describing displacements of the more loosely coordinated axial ligands. In general, up to five sets of dynamical parameters are required to describe the distortions of a quadratic Hamiltonian, $H_{ZFS,T}(t)$, without (P) frame symmetry, corresponding to the five Cartesian tensor components ($q=1 \cdots 5$ for z^2 , x^2-y^2 , xz , yz , and xy). The molecular dynamics of collisional distortions are also complex, involving random large step motions rather than the

classical diffusion picture used to describe molecular translation and reorientation. And finally, for $S > 1/2$, electron spin relaxation is in general multiexponential, i.e., the decay depends on spin eigenstates.

The theory derived in Ref. 42 addresses some of these concerns. Specifically, the formalism incorporates the five quadratic degrees of freedom and computes the full set of eigenstate-dependent relaxation rates using a Redfield theory (this requires $\Delta_T \tau_i < 1$). The calculation is valid for a permanent ZFS tensor of any magnitude or symmetry.

In practice, such detailed physical parametrization is seldom justified by the available information. What is needed is a description of the collisional mechanism that is comparable to Bloembergen-Morgan theory with respect to the complexity of the physical description (i.e., a single set of parameters, Δ_T and τ_i , is used to calculate two eigenstate-averaged relaxation rates, τ_{S1}^{-1} and τ_{S2}^{-1} , along the z and x laboratory axes) but which accounts for the effects of the permanent ZFS Hamiltonian in Eq. (12). The following closed form expressions for these quantities are derived in Ref. 43:

$$(\tau_{S,r})^{-1} = [S(S+1)/3]^{-1} (2S+1)^{-1} (\Delta_T^2/5) \times \sum_{q=1}^5 n_q^{(r)} \sum_{\mu,\nu} \{ \langle \mu | S_q^{(2)} | \nu \rangle \}^2 k(\omega_{\mu\nu}), \quad (34)$$

$$k(\omega) = \tau_i / (1 + \omega^2 \tau_i^2). \quad (35)$$

The matrix elements in Eq. (34) are evaluated in the eigenbasis, $\{\mu, \nu\}$, of $H_S^\circ(\alpha, \beta, \gamma, t)$, for which $\omega_{\mu\nu}$ are transition frequencies. The quantities $S_q^{(2)}$ are the five quadratic Cartesian tensor functions of the spin operators which transform spatially like the d orbitals ($q=1-5$ signify z^2, x^2-y^2, xz, yz, xy). The quantities $n_q^{(r)}$ are integer coefficients which arise in the calculation of the double commutators of the spin operators.⁴³ The curly brackets indicate an average over molecular orientations.

G. The implementations

To make the section complete, the three methods are discussed hereafter in terms of easiness of implementation, computer efficiency, and possible generalization to more complex systems.

The S method is based on expressing the lattice Liouvillean as a (super)matrix in a vector space defined by a suitable set of lattice operators. These operators are products of an electron spin part and Wigner rotation matrices of Euler angles describing the orientation of the P_S and P_T frames in the laboratory frame.^{38,44} The size of the vector space depends on the maximum L quantum numbers for the Wigner matrices considered. If the largest L values for rotation and pseudorotation are set to eight, which is sufficient in most cases of practical interest, then the dimensionality of the vector space is about 30 000 for $S=1$ and about 200 000 for $S=7/2$. The computationally heavy step is finding a small number of elements of the inverse of the complex matrix representing the lattice Liouvillean. This is carried out efficiently using the Lanczos algorithm, with a single point calculation for most cases requiring less than a minute on a

modern single-processor work station. The S method can be extended to include other terms in the perturbation, the one that we work on at present is the anisotropy of the g_S tensor. More complex dynamics is in principle possible to handle, but at the expense of larger matrices representing the lattice Liouvillean.

The G method is based on the statistics of an ensemble of spin systems which are submitted to fluctuating Hamiltonians and the quantum states of which have an evolution that is directly obtained by solving the time-dependent Schrödinger equation numerically. The equations are simple, but have to be translated into an efficient computer code on a single processor. Then, parallel programming is rather straightforward since all the spin systems can be handled on the same footing. The numerical work just scales with the size of the Hamiltonian matrices to be diagonalized. On a fast single-processor personal computer, the calculation of the PRE at a given field requires typically 3 and 12 min for $S=1$ and $S=7/2$, respectively, to reach a statistical convergence to within 1%. According to the crudeness of the ZFS models, an accuracy of 5% is generally sufficient for practical applications and then, the above times are reduced by a factor of 25. The computational load comes mainly from the evaluation of the evolution operator, so that it only slightly increases with the number of nuclei located on the complex and corresponding to various θ values.

For a slow tumbling of the metal complex, it may be problematic when the relaxation magnetic field increases beyond 2.35 T since the dipolar local field TCF to be integrated shows a slower and slower decay with faster and faster oscillations around 0. The numerical work becomes also heavier for large ZFS parameters Δ_S , $\Delta_T \geq 10 \text{ cm}^{-1}$ as the time step of integration Δt has to be significantly shorter than $2\pi/\Delta_S$ and $2\pi/\Delta_T$. However, at sufficiently high field, it was shown recently²¹ that the longitudinal electronic relaxation decays monoexponentially at a rate given by the Bloembergen and Morgan equation, Eq. (15). This leads to the simple and accurate expression of the PRE, Eq. (31).

The G method can be easily extended to ZFS Hamiltonians including second order rhombic terms and contributions of fourth and sixth order in the case of gadolinium complexes. It is also suitable to deal with coupled electronic spins. More complex intramolecular dynamics, such as Brownian anisotropic rotation and/or constrained reorientation, can also be modeled.

The AA method is implemented in the computer program PARELAX2, which consists of a suite of four formulations of theory.⁵¹ One of these, SD simulation, was used in the present calculations. It is broadly similar to the G method except with respect to the calculation of electron spin relaxation times, for which the Redfield Theory of Ref. 54 is used. The Redfield description incorporates a more realistic force field for the ZFS distortional motions than does pseudorotation, but it is limited in its range of validity by the Redfield criterion, $\Delta_T \tau_p < 1$. However, both of these treatments are highly simplified, and a realistic, quantitative description of electron spin relaxation in general physical systems remains a formidable problem, even given the computational power that is now available.

The other modules of PARELAX2 are based on the “constant H_S ” approximation; i.e., they ignore the reorientational motion of the permanent ZFS Hamiltonian when computing the electron spin TCF. The principal advantage of constant H_S formulations is that they provide a physically transparent picture of the relaxation mechanism in terms of the oscillatory motions of specific spin matrix elements. Also, constant H_S provides a suitable platform for the incorporation of eigenstate-specific electron spin relaxation times while SD does not. Each approach has advantages and drawbacks, none providing an entirely satisfactory description of the relaxation process. In practice, the four formulations are used in a complementary manner to provide as full a picture of the relaxation mechanism as possible.

III. RESULTS AND DISCUSSION

We perform the calculations for two classes of complexes, with two different electron spin quantum numbers. Besides the parameters discussed in Sec. II C and the spin quantum number, we also need to specify the dipole-dipole coupling constant. Since it only acts as a scaling factor for the profile, the choice of a suitable value is not critically important for the comparison of methods. We set the dipole-dipole coupling constant equal to 16.7 MHz, corresponding to $g_S=2.0023$ and $r_{IS}=310 \text{ pm}$.

The case of $S=7/2$ is meant to correspond to Gd(III) complexes. Because of the highly symmetric electronic distribution, with the $(4f)^7$ configuration of the lanthanide providing the highly stable 8S ground state term with fully quenched orbital angular momentum, the ZFS can only reach very low values.⁵⁷ We have done the calculations for the following ZFS parameters,

$$\Delta_S = 0.01, 0.03, 0.05 \text{ cm}^{-1},$$

$$\Delta_T = 0.01, 0.05 \text{ cm}^{-1}.$$

Two types of complexes were considered, a very large complex characterized by the rotational correlation time of $\tau_R = 1 \mu\text{s}$, and a rather small one with $\tau_R = 100 \text{ ps}$. The distortional correlation time was set to a value of 5 ps. Likewise, two values were used for the angle, between the principal axes of the static ZFS and the dipole-dipole interactions, $\theta = 0^\circ$ and 90° .

We begin the discussion from the case of the long rotational correlation time $\tau_R = 1 \mu\text{s}$. For slowly rotating molecular systems, i.e., with electronic relaxation time $T_{1e} \ll \tau_R$, the electron spin relaxation is the only source of the modulations of the I - S dipole-dipole interaction. If the static ZFS dominates over the transient counterpart, the energy level structure of the electron spin is defined by a superposition of the static ZFS and the Zeeman interaction.^{36,37} In this case, if the transient ZFS fulfills the Redfield condition, $\Delta_T \tau_p \ll 1$, the electron spin relaxation rates are well defined within the second order perturbation theory. The parameter sets, $\Delta_T = 0.01 \text{ cm}^{-1}$, $\Delta_S = 0.03 \text{ cm}^{-1}$, and $\theta = 0^\circ$ or $\theta = 90^\circ$, fulfill the requirements. The relaxation profiles for these parameters are presented in Figs. 2(a) and 2(b). The figures present the relaxation profiles predicted by the slow motion theory (S), the

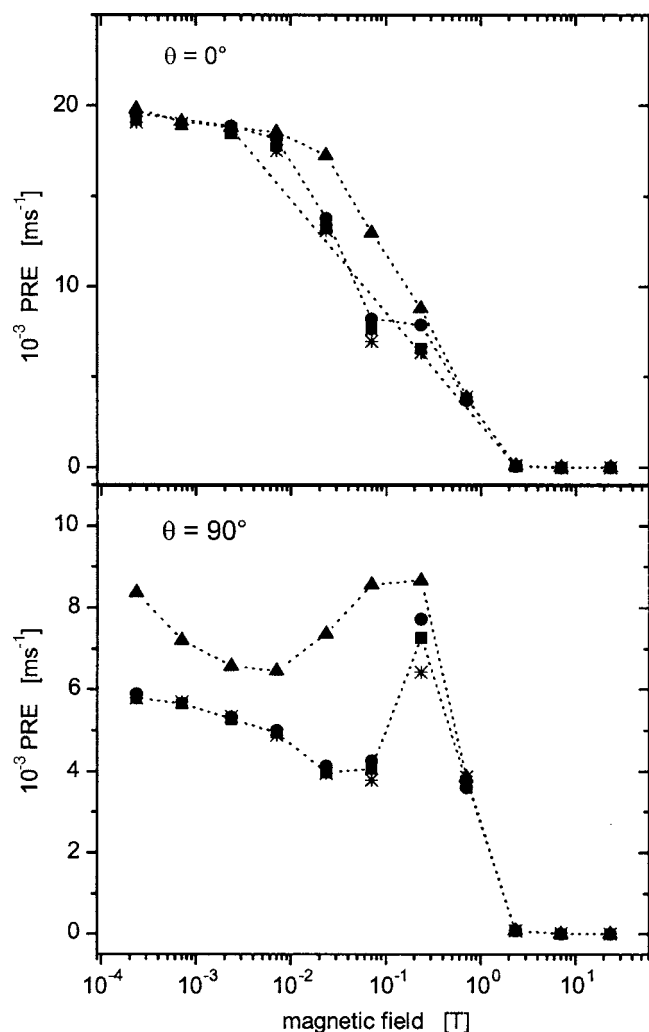


FIG. 2. Proton relaxation profiles for the electron spin quantum number $S = 7/2$ and slow molecular tumbling $\tau_R = 1 \mu\text{s}$. The ZFS parameters are $\Delta_S = 0.03 \text{ cm}^{-1}$ and $\Delta_T = 0.01 \text{ cm}^{-1}$. (▲) the Ann Arbor method, (●) the Swedish slow motion method, (■) the Grenoble method, and (*) the Florence method.

Grenoble approach (G), and the Ann Arbor approach (AA). We can see that the S and G methods agree with each other within few percent for all magnetic fields. For $\theta = 0^\circ$, the AA method agrees with the other two at the high field and the low field limits, but deviates significantly for intermediate fields. For $\theta = 90^\circ$, the AA method agrees with the other ones only at high field. In these cases, the physical situation is rather simple and the differences between the S and G approaches on the one hand and the AA method on the other can be traced to differences in the treatment of electron spin relaxation. Two features of the AA model deviate from the other two approaches. One is the use of level-specific or level-averaged relaxation in the thermal ensemble proposed by Sharp and Lohr⁴² and Sharp⁴³ and implemented in the AA approach. Another specific feature of the AA approach is the use of orientationally averaged electron spin relaxation times, in the spin relaxation function applied in the SD simulation.

The S theory does not include any explicit description of the electron spin relaxation and, therefore, one does not profit here from the fact that the perturbation theory applies

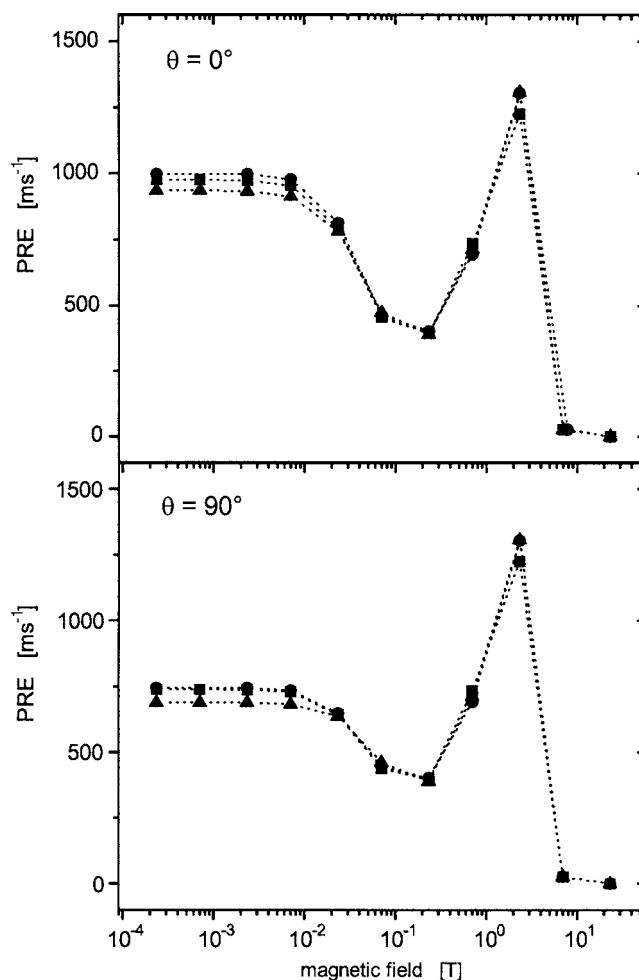


FIG. 3. Proton relaxation profiles for the electron spin quantum number $S = 7/2$ and slow molecular tumbling $\tau_R = 1 \mu\text{s}$. The ZFS parameters are $\Delta_S = 0.01 \text{ cm}^{-1}$ and $\Delta_T = 0.05 \text{ cm}^{-1}$. (▲) the Ann Arbor method, (●) the Swedish slow motion method, and (■) the Grenoble method.

in principle to the electron spin subsystem (this feature is available in the time-domain version^{45,46}). The perturbation description of the electron spin relaxation (i.e., the Redfield theory) has been incorporated into the so-called “modified Florence approach” (F).^{36,37} This method can deal with slowly rotating systems at arbitrary magnetic field and static ZFS, if the transient ZFS is smaller than the static ZFS as discussed previously⁵⁸ and if the electron spin relaxation is within the Redfield limit. This approach, when its validity conditions are fulfilled, has earlier been shown to agree with the Swedish slow motion theory.^{36,37} The results of this treatment are included in Fig. 2 (and its counterpart in the supplementary material⁵⁹). As expected, the agreement is good between the S and the F methods.⁶⁰

The relaxation profiles obtained when the transient ZFS is comparable to or larger than its static counterpart are presented next. Figure 3 shows the proton relaxation rates calculated for the electron spin quantum number $S = 7/2$ and the following parameters: $\Delta_T = 0.05 \text{ cm}^{-1}$, $\Delta_S = 0.01 \text{ cm}^{-1}$, $\theta = 0^\circ$, and $\theta = 90^\circ$. Here, the S, G, and AA methods agree quite closely. The close agreement between the three approaches in this case may perhaps be related to the fact that averaging over orientations plays a smaller role with the low static

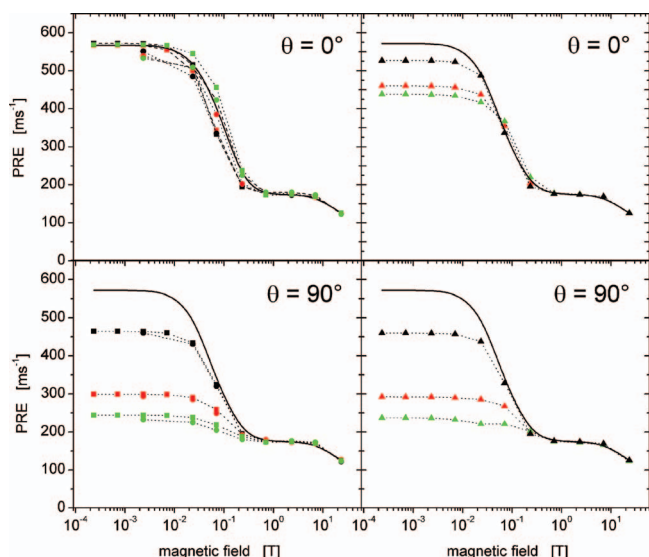


FIG. 4. (Color) Proton relaxation profiles for the electron spin quantum number $S=7/2$ and fast molecular tumbling $\tau_R=100$ ps. The transient ZFS parameter is $\Delta_T=0.01$ cm^{-1} , each graph shows the profiles for varying Δ_S . (Left) The Swedish method, black squares: $\Delta_S=0.01$ cm^{-1} , red squares: $\Delta_S=0.03$ cm^{-1} , green squares: $\Delta_S=0.05$ cm^{-1} , and (—): $\Delta_S=0$ (the Zeeman expression) and the Grenoble method, black circles: $\Delta_S=0.01$ cm^{-1} , red circles: $\Delta_S=0.03$ cm^{-1} , and green circles: $\Delta_S=0.05$ cm^{-1} . (Right) The Ann Arbor approach, black triangles: $\Delta_S=0.01$ cm^{-1} , red triangles: $\Delta_S=0.03$ cm^{-1} , green triangles: $\Delta_S=0.05$ cm^{-1} , and (—): $\Delta_S=0$ (the Zeeman expression). Note that the PRE curves decrease with increasing Δ_S for $\theta=90^\circ$ and in case of the Ann Arbor method also for $\theta=0^\circ$.

ZFS. The F method was not applied in this case, as one of its validity conditions is not fulfilled at low field,⁵⁸ while one could expect it to work at the high field limit. The remaining NMRD profiles for slowly rotating $S=7/2$ systems are shown in Ref. 59 (Figs. S1–S4).

Faster molecular tumbling makes the problem of the electron spin dynamics (and, in consequence, the nuclear spin relaxation) more complicated. With $\tau_R=100$ ps, our range of parameters (used for $S=7/2$) corresponds to the region of motional collapse of the (static) ZFS level structure: For $\Delta_S=\{0.01, 0.03, 0.05\}$, we have $\Delta_S\tau_R=\{0.2, 0.6, 1\}$. When $\Delta_S\tau_R \ll 1$, the ZFS level structure averages to zero and the result is equivalent to the Zeeman limit, even at low field. The relaxation effects of the rotational modulation of the permanent ZFS can then be taken into account by Redfield-type approach, along with the collisional mechanism.²⁰ As Δ_S or τ_R increases so that the level structure is not motionally averaged, the situation becomes more complicated and, except for few limiting cases,^{58,61,62} one cannot treat the electron spin dynamics within the perturbation theory. The relaxation profiles obtained for the rotational correlation time $\tau_R=100$ ps and the low transient ZFS ($\Delta_T=0.01$ cm^{-1}) and varying static ZFS are presented in Fig. 4. For $\theta=0^\circ$, there is an interesting qualitative difference between the predictions of the S and G models (left panels in Fig. 4), on the one hand, and the AA model (right panels in Fig. 4) on the other. According to the S and G approaches, the PRE at low field is independent of the magnitude of the static ZFS when the principal axis of that tensor coincides with the DD principal axis ($\theta=0$) (cf. upper left panel in Fig. 4). To the contrary, the AA approach predicts a smooth decrease of the low-field

PRE with increasing Δ_S (upper right panel in Fig. 4). This latter trend can be given by the following physical explanation, within the AA way of thinking. In the range of assumed Δ_S values (0.01 – 0.05 cm^{-1}), the ZFS level structure is partially collapsed by molecular reorientation (note that $\Delta_S\tau_R=0.2$ when $\Delta_S=0.01$ cm^{-1} and $\Delta_S\tau_R=1$ when $\Delta_S=0.05$ cm^{-1}). At $\Delta_S=0.05$ cm^{-1} , the motional averaging of the level structure is less efficient. The collapse of ZFS level structure in the low field region is accompanied by a change in electron spin wavefunction. When $\Delta_S\tau_R \ll 1$, the spin wavefunctions are Zeeman functions with a laboratory polarization. This is true even at the lowest field strengths where the ZFS exceeds the Zeeman interaction. With increasing Δ_S , the low field spin wavefunctions change from Zeeman-limit functions having a laboratory polarization (at small Δ_S) to ZFS-limit functions with a molecule-fixed polarization (at large Δ_S). This change in spin wavefunction with increasing Δ_S is accompanied by profound changes in spin physics, involving both a change of spatial quantization of the spin motion (from laboratory to molecule fixed) and changes in the spin dynamics (i.e., changes of the spin eigenfrequencies). The calculated AA profiles result from these changes in the spin physics.

The lack of the ZFS dependence of the low-field PRE, obtained in the S and G calculations, has been noticed already in the early Swedish slow-motion theory papers, not including the transient ZFS.^{25,63,64} This observation can be given the following physical interpretation, within the S way of thinking. When the static ZFS dominates over the Zeeman interaction the electron spin becomes locked in the ZFS frame. When there are no other sources of electron spin relaxation, the rotation of this frame with respect to the laboratory is the only source of modulation of the DD interaction between the electron and nuclear spins. Since the static ZFS and the dipole-dipole interactions are entirely modulated by the same stochastic motion (the rotation), cross-correlation effects between them becomes relevant. The magnitude of this cross-correlation effect depends on the relative orientation of the principal axis system of the ZFS tensor and the DD axis. For the case of $\theta=0^\circ$ the cross correlation exactly cancels the dependence of the nuclear spin relaxation on the static ZFS (Refs. 63 and 64) (if there is no transient ZFS), while for $\theta \neq 0^\circ$ some effects of the static ZFS remain. With the present parameter values, the electron spin relaxation is much slower than rotation and the physical description above remains largely valid. The G method perceives this phenomenon, whereas, apparently, the AA approach does not. We can also see in the lower panels in Fig. 4 that the locking effect does not occur for $\theta=90^\circ$, where the S, G, and AA approaches behave very similarly. A reasonable explanation of this observation is that for $\theta \neq 0^\circ$, the cross correlation of the static ZFS and the DD interaction is reduced while the static ZFS effects discussed above remain effective.⁶⁵

The case of fast rotation and larger transient ZFS ($\Delta_T=0.05$ and $\Delta_S=0.01$ cm^{-1}) is presented in Fig. 5. Here, the electron spin relaxation is more efficient and the three methods follow each other quite closely. The remaining profiles for fast rotating $S=7/2$ systems are collected in the Figs. S5–S6 in Ref. 59.

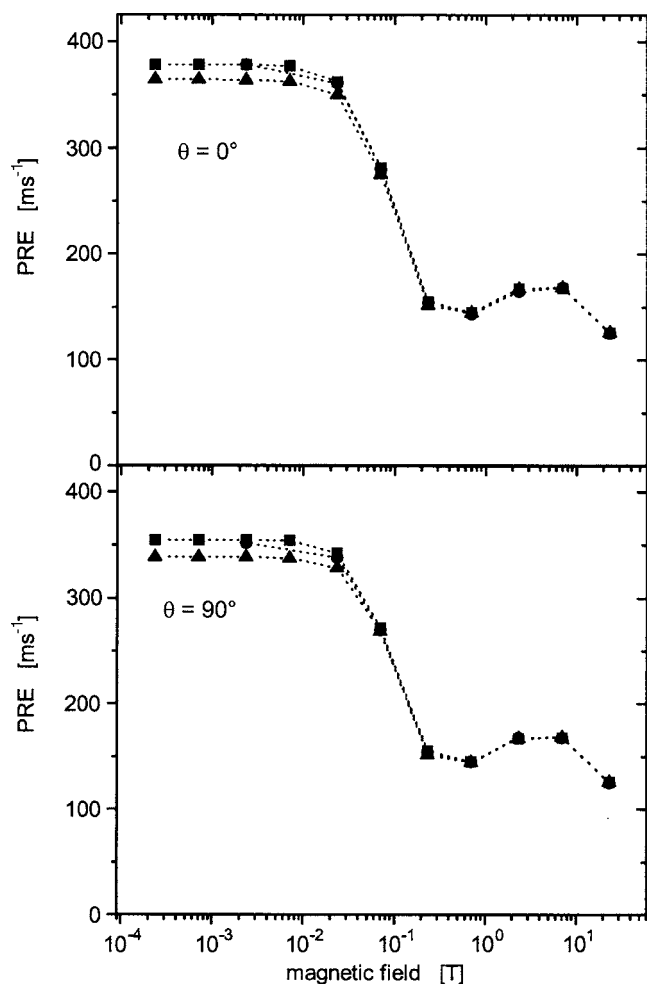


FIG. 5. Proton relaxation profiles for the electron spin quantum number $S = 7/2$ and fast molecular tumbling $\tau_R = 100$ ps. The ZFS parameters are $\Delta_S = 0.01$ cm^{-1} and $\Delta_T = 0.05$ cm^{-1} (\blacktriangle) the Ann Arbor method, (\blacksquare) the Swedish slow motion method, and (\bullet) the Grenoble method.

The case of $S=1$ is meant to correspond to Ni(II) complexes. This transition metal ion is characterized by the electron configuration $(3d)^8$ with the 3F ground state term. Here, the ZFS is typically much larger,⁵⁷ which easily brings the Ni(II) complexes out of the Redfield limit for the electron spin relaxation. We have here done the calculations for the following ZFS parameters,

$$\Delta_S = 1, 3, 10 \text{ cm}^{-1},$$

$$\Delta_T = 1, 10 \text{ cm}^{-1}.$$

For the dipolar coupling strength, correlation times and the θ angle, we have used the same values as above for the $S = 7/2$ case.

The $S=1$ systems with $\Delta_T = 1$ cm^{-1} seem near the edge of the region of validity of the Redfield approximation, which may be a source, to a greater or lesser degree, of differences in the calculated results. The calculations with $\Delta_T = 10$ cm^{-1} , i.e., $\Delta_T \tau_v \cong 10$, are out of the range of validity of the Redfield theory, and thus of the AA approach, so that they can be considered more demanding. This will be established by comparing the results of the three methods. The relaxation profiles predicted by the three discussed ap-

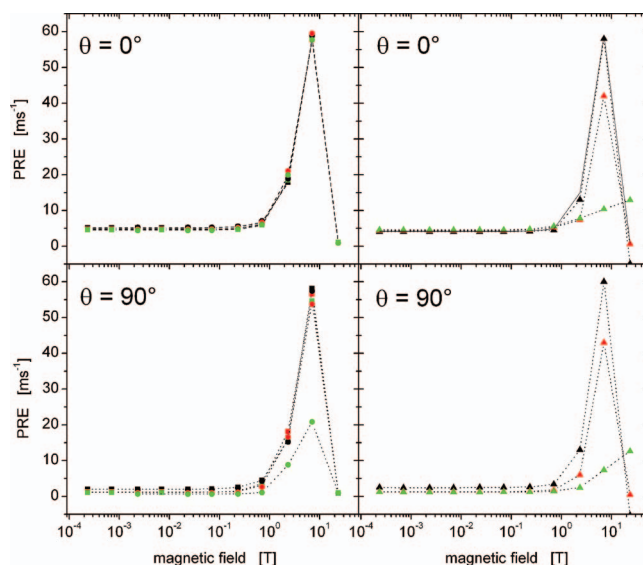


FIG. 6. (Color) Proton relaxation profiles for the electron spin quantum number $S=1$ and slow molecular tumbling $\tau_R = 1$ μs . The transient ZFS parameter is $\Delta_T = 1$ cm^{-1} ; each graph shows the profiles for varying Δ_S . (Left) The Swedish method, black squares: $\Delta_S = 1$ cm^{-1} , red squares: $\Delta_S = 3$ cm^{-1} , green squares: $\Delta_S = 10$ cm^{-1} and the Grenoble method, black circles: $\Delta_S = 1$ cm^{-1} , red circles: $\Delta_S = 3$ cm^{-1} , green circles: $\Delta_S = 10$ cm^{-1} . (Right) The Ann Arbor approach, black triangles: $\Delta_S = 1$ cm^{-1} , red triangles: $\Delta_S = 3$ cm^{-1} , green triangles: $\Delta_S = 10$ cm^{-1} , and (—) $\Delta_S = 0$ (the Zeeman expression).

proaches (the slow motion theory, the Grenoble approach, and the Ann Arbor approach) for the parameter values $\Delta_T = 1.0$ cm^{-1} , $\Delta_S = 1, 3, 10$ cm^{-1} , and $\tau_R = 1$ μs , are presented in Fig. 6 for the angles $\theta = 0^\circ$ and $\theta = 90^\circ$. This kind of complexes has been called in Swedish studies slightly deformable (relatively small transient ZFS), with variable asymmetry (small to large static ZFS).⁴⁴ For $\theta = 0^\circ$, the three methods agree quite well at low magnetic fields, up to about 0.5 T (where the electron Zeeman splitting is less or approaching to the static ZFS), for all Δ_S values. At higher magnetic field strengths, the S and G approaches give similar results, which differ significantly from those of the AA method. The S and G profiles remain essentially identical to the Zeeman-limit profile when Δ_S varies from 0 to 10 cm^{-1} . In contrast, the AA method predicts that the high-field (1–10 T) relaxivity depends strongly on the magnitude of Δ_S , decreasing as Δ_S increases from 1 to 10 cm^{-1} . In this physical regime of field strengths and ZFS couplings (1–10 T, 1–10 cm^{-1}), the Zeeman energy is comparable to the static ZFS energy, and in consequence, both the electron spin wavefunctions and the electron spin level structure depend strongly on the relative magnitudes of the Zeeman and ZFS energies. In the AA calculation, the electron spin dynamics depend profoundly on the changes in spin physics which occur in this physical regime, and the altered spin dynamics are reflected in the behavior of the NMR-PRE.

This argumentation does not seem to apply to the G and S results. A possible explanation may again be sought in the electron spin relaxation effects. As discussed by Bertini *et al.*,³⁶ for another set of parameters within the same physical range, the electron spin relaxation at high field and for sizable static ZFS becomes quite intricate, with several indi-

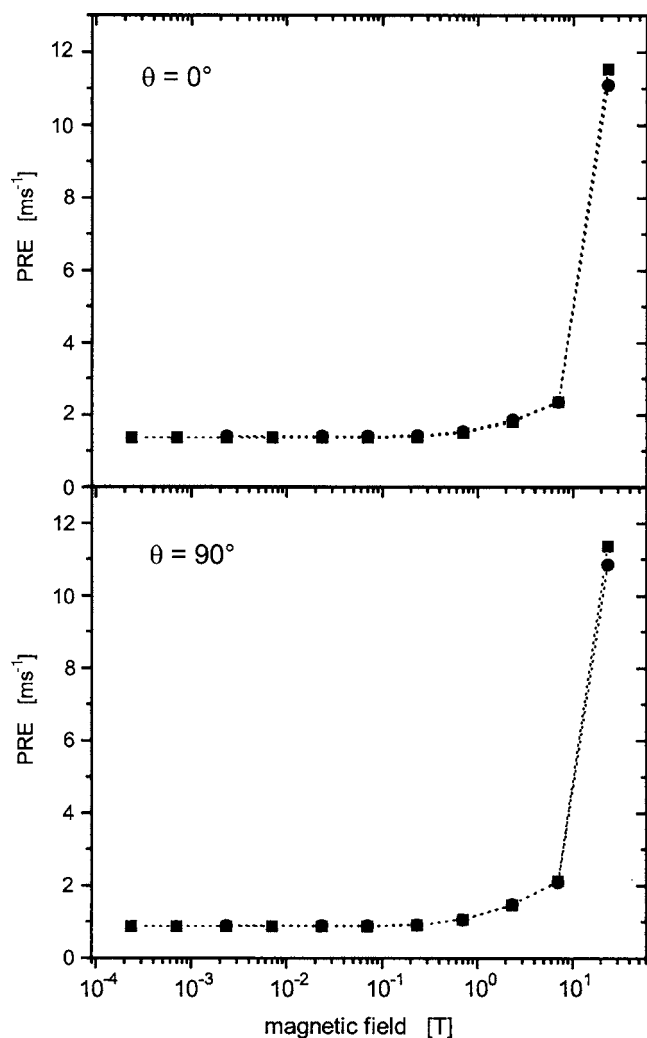


FIG. 7. Proton relaxation profiles for the electron spin quantum number $S = 1$ and slow molecular tumbling $\tau_R = 1 \mu\text{s}$. The ZFS parameters are $\Delta_S = 1.0 \text{ cm}^{-1}$ and $\Delta_T = 10 \text{ cm}^{-1}$. (■) The Swedish slow motion method and (●) the Grenoble method.

vidual rate processes contributing to the PRE. It may be so that these electron spin relaxation effects somehow offset the AA argumentation above.

For $\theta = 90^\circ$ (again with $\Delta_T = 1 \text{ cm}^{-1}$ and $\tau_R = 1 \mu\text{s}$), the three calculations (S, G, and AA) give very similar results in the low field region. In the high field region, the S/G profiles differ greatly from those of AA, reflecting again the differences discussed in the preceding paragraph. Moreover, the $\Delta_S = 10 \text{ cm}^{-1}$ case is the only one in this study where the S and G approaches give results that differ significantly from each other. The origin of this discrepancy is not quite clear.

Figure 7 shows the nuclear spin relaxation profiles for slowly rotating $S = 1$ for the case of transient and static ZFS changing places and becoming: $\Delta_T = 10 \text{ cm}^{-1}$ and $\Delta_S = 1.0 \text{ cm}^{-1}$ (slightly asymmetric and highly deformable complex). The large transient ZFS does not allow for a perturbation treatment of the electron spin, as it has been already pointed out. The S and G approaches agree here very well. The Ann Arbor approach predicts PRE values (not shown) which can be more than one order of magnitude too small and is thus not applicable for $\Delta_T = 10 \text{ cm}^{-1}$ as described

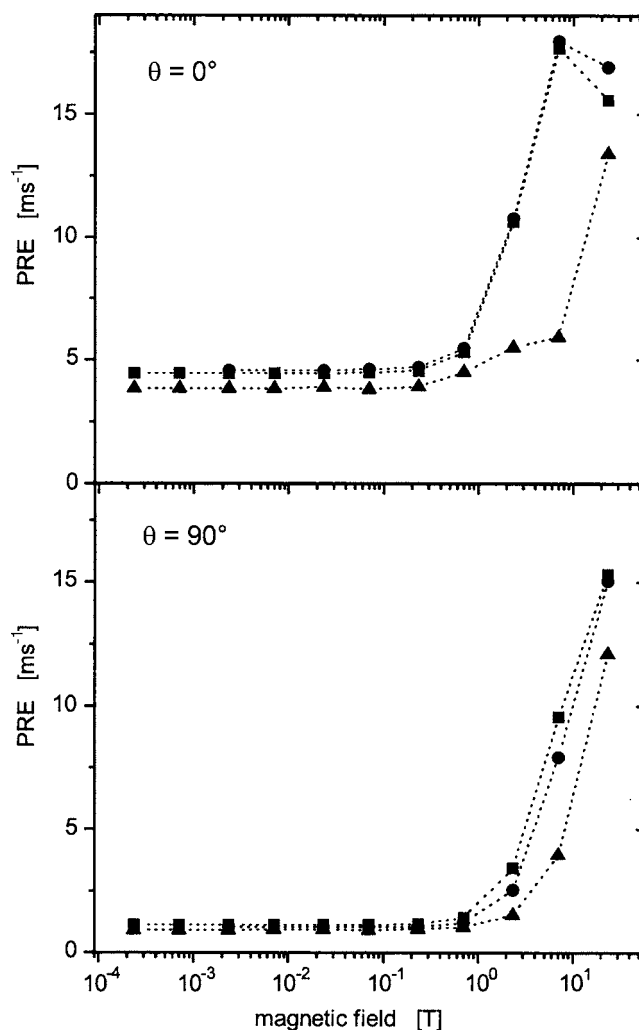


FIG. 8. Proton relaxation profiles for the electron spin quantum number $S = 1$ and fast molecular tumbling $\tau_R = 100 \text{ ps}$. The ZFS parameters are $\Delta_S = 10 \text{ cm}^{-1}$ and $\Delta_T = 1.0 \text{ cm}^{-1}$. (▲) The Ann Arbor method, (■) the Swedish slow motion method, and (●) the Grenoble method.

above. It should be kept in mind, however, that the parameter values in this range are expected to be uncommon. The remaining relaxation profiles obtained for slowly rotating, $S = 1$ systems are collected in Ref. 59 as Figs. S7–S8.

Finally, we present in the last two figures the NMRD profiles for rapidly rotating $S = 1$ cases. Figure 8 shows the case of highly asymmetric, slightly deformable complex ($\Delta_T = 1.0 \text{ cm}^{-1}$ and $\Delta_S = 10 \text{ cm}^{-1}$) with $\tau_R = 100 \text{ ps}$. Also in this case, the differences between the S and G methods are at most a few percent, while the AA results deviate. In Fig. 9, we display the results of calculations for a slightly asymmetric and highly deformable complex ($\Delta_T = 10 \text{ cm}^{-1}$ and $\Delta_S = 1.0 \text{ cm}^{-1}$) with $\tau_R = 100 \text{ ps}$. Here again, the results of the S and G methods are very close to each other. The other relaxation profiles for fast rotating $S = 1$ systems are collected in Ref. 59 as Figs. S9–S12.

IV. CONCLUSIONS

Summarizing the above discussion, it can be stated that there is an overall very satisfactory agreement between the results obtained by the apparently very different Swedish and

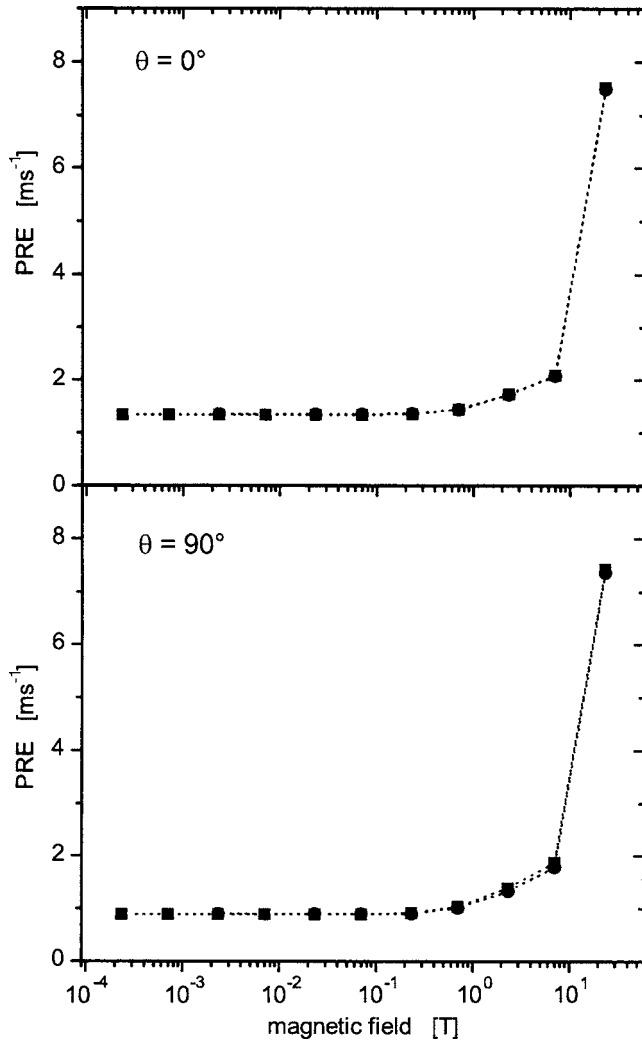


FIG. 9. Proton relaxation profiles for the electron spin quantum number $S = 1$ and fast molecular tumbling $\tau_R = 100$ ps. The ZFS parameters are $\Delta_S = 1.0 \text{ cm}^{-1}$ and $\Delta_T = 10 \text{ cm}^{-1}$. (■) The Swedish slow motion method and (●) the Grenoble method.

Grenoble techniques, with the exception of the uncommon situation of a very large static ZFS $\Delta_S = 10 \text{ cm}^{-1}$, a very slow rotation $\tau_R = 1 \text{ } \mu\text{s}$, $\theta = 90^\circ$ (one case among 48 investigated systems!)

This very satisfactory agreement was expected since the S and G approaches use the same physical model of molecular motion and ZFS fluctuations, and compute the PRE due to the nuclear-electronic dipolar Hamiltonian with the help of mathematical treatments, which are different, but exact to within numerical accuracy. The AA approach was designed to deal with more realistic models of the transient ZFS inducing the electronic spin relaxation, which is described within the Redfield approximation, whereas the electronic spin dynamics due to the Zeeman and static ZFS Hamiltonians is solved rigorously. When this Redfield approximation holds, the AA predictions for the simple physical model studied here are close to the S and G results in many cases, even if subtle differences are observed.

ACKNOWLEDGMENTS

This work originates from a couple of meetings organized by Lothar Helm under the auspices of the EC COST

Action D-18 “Lanthanide Chemistry for Diagnosis and Therapy.” The research described has been supported by the Swedish Research Council, the EC COST Action D-38 “Metal-Based Systems for Molecular Imaging Applications,” the European Molecular Imaging Laboratories (EMIL) network, and the CERM infrastructure access program (EU-NMR, Contract No. RII3-026145). Valuable discussions with Professor Claudio Luchinat and Professor Giacomo Parigi are gratefully acknowledged.

APPENDIX: PRACTICAL EVALUATION OF THE PARAMAGNETIC RELAXATION ENHANCEMENT WITHIN THE GRENOBLE APPROACH

From Eqs. (26) and (27), the initial value of the TCF $k_{-1}(t)$ of the dipolar local field is

$$k_{-1}(0) = \left(\frac{\mu_0}{4\pi} \right)^2 \frac{2}{3} g_S^2 \mu_B^2 S(S+1) \frac{1}{r_{IS}^6}. \quad (\text{A1})$$

We define the normalized TCF of the dipolar local field as

$$k_{-1}^{\text{nor}}(t) \equiv k_{-1}(t)/k_{-1}(0). \quad (\text{A2})$$

In the general case the expression of the PRE in Eq. (28) is computed by integrating the simulated TCF $k_{-1}(t)$ over a finite time interval $[0, t_{\text{max}}]$,

$$\begin{aligned} \text{PRE} &\equiv 1/T_{1M} \equiv 2\gamma_I^2 \text{Re} \int_0^\infty k_{-1}(t) \exp(-i\omega t) dt \\ &\equiv 2\gamma_I^2 k_{-1}(0) \int_0^{t_{\text{max}}} \text{Re}[k_{-1}^{\text{nor}}(t) \exp(-i\omega t)] dt, \end{aligned} \quad (\text{A3})$$

where the upper bound t_{max} is chosen such as $k_{-1}^{\text{nor}}(t_{\text{max}}) < 0.01$ is approximated by 0. The numerical integration is carried out with the help of the trapezoidal rule with n_t equally spaced integration points $t_p \equiv (p-1)\Delta t$ ($1 \leq p \leq n_t$) and $t_{\text{max}} = (n_t - 1)\Delta t$, so that

$$\begin{aligned} \text{PRE} &\equiv 2\gamma_I^2 \Delta t \left\{ -0.5k_{-1}(0) + \sum_{p=1}^{n_t} \text{Re}[k_{-1}(t_p)] \right. \\ &\quad \left. \times \exp(-i\omega t_p) \right\}. \end{aligned} \quad (\text{A4})$$

According to the discussion after Eq. (28), the TCF $k_{-1}(t)$ can be approximated by the high-field expression

$$k_{-1}^{\text{high field}}(t) = \frac{3}{10} k_{-1}(0) \exp(-t/\tau_R) G_{\parallel}^{\text{nor}}(t), \quad (\text{A5})$$

where the normalized (nor) longitudinal TCF of the electronic spin defined as

$$G_{\parallel}^{\text{nor}}(t) \equiv \langle S_z(t) S_z(0) \rangle / \langle S_z(0) S_z(0) \rangle \quad (\text{A6})$$

has the monoexponential decay

$$G_{\parallel}^{\text{nor}}(t) = \exp(-t/T_{1e}), \quad (\text{A7})$$

with $1/T_{1e}$ given by Eqs. (15) and (19). According to Eqs. (A2), (A5), and (A7), the high-field normalized TCF of the dipolar local field is

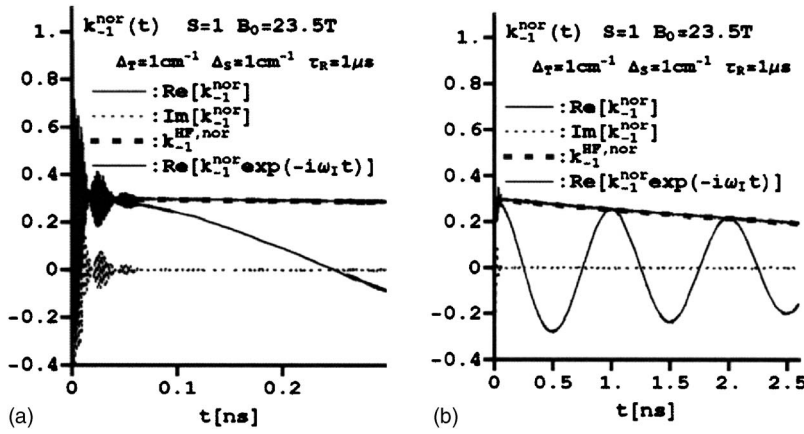


FIG. 10. $S=1$ and $B_0=23.5$ T. The decay of the Monte Carlo simulated TCF $k_{-1}^{nor}(t)$ of the dipolar local field in the case of a slow tumbling $\tau_R=1 \mu\text{s}$. The ZFS parameters are $\Delta_S=\Delta_T=1 \text{ cm}^{-1}$ and the relative orientation angle is $\theta=0$. The functions $\text{Re}[k_{-1}^{nor}(t)]$ and $\text{Re}[k_{-1}^{nor}(t)\exp(-i\omega_I t)]$ are both represented by continuous lines. As the time t increases, $\text{Re}[k_{-1}^{nor}(t)]$ tends to the slowly decaying exponential $k_{-1}^{\text{high field, nor}}(t)$, whereas $\text{Re}[k_{-1}^{nor}(t)\exp(-i\omega_I t)]$ to be integrated for calculating the PRE displays many oscillations over the decay period of $\text{Re}[k_{-1}^{nor}(t)]$. (a) Short-time behavior and (b) long-time decay.

$$k_{-1}^{\text{high field, nor}}(t) \equiv k_{-1}^{\text{high field}}(t)/k_{-1}(0) = \frac{3}{10} \exp(-t/\tau_R)\exp(-t/T_{1e}). \quad (\text{A8})$$

Defining the correlation time τ_{c1} by $1/\tau_{c1} \equiv 1/\tau_R + 1/T_{1e}$, the high-field PRE is given by

$$\begin{aligned} \text{PRE}^{\text{high field}} &\equiv 1/T_{1M}^{\text{high field}} \\ &\equiv 2\gamma_I^2 \int_0^\infty k_{-1}^{\text{high field}}(t) \cos(\omega_I t) dt \\ &\equiv 2\gamma_I^2 k_{-1}(0) \int_0^\infty k_{-1}^{\text{high field, nor}}(t) \cos(\omega_I t) dt \\ &= \left(\frac{\mu_0}{4\pi}\right)^2 \frac{2}{5} \gamma_I^2 g_S^2 \mu_B^2 S(S+1) \frac{1}{r_{IS}^6} \frac{\tau_{c1}}{1 + \omega_I^2 \tau_{c1}^2}. \end{aligned} \quad (\text{A9})$$

These high-field properties are illustrated in Fig. 10 for one representative situation considered in this work, $S=1$, $\Delta_S=\Delta_T=1 \text{ cm}^{-1}$, $\theta=0$, $\tau_R=1 \mu\text{s}$, and $\tau_v=5 \text{ ps}$. After a short transient oscillatory period, the real part $\text{Re}[k_{-1}^{nor}(t)]$ of $k_{-1}^{nor}(t)$ tends to the exponential function $k_{-1}^{\text{high field, nor}}(t)$ which decays slowly with a characteristic time $\tau_{c1} \approx T_{1e}$, while its imaginary part $\text{Im}[k_{-1}^{nor}(t)]$ tends to zero. The transient oscillations of $\text{Re}[k_{-1}^{nor}(t)]$ and $\text{Im}[k_{-1}^{nor}(t)]$ around the “long”-time limits $k_{-1}^{\text{high field, nor}}(t)$ and 0 have negligible effects on the value Eq. (A3) of the PRE, which simplifies to Eq. (A9). Such a simplification is particularly useful. Indeed, calculating the integral Eq. (A3) of $\text{Re}[k_{-1}^{nor}(t)\exp(-i\omega_I t)]$ is computer demanding since it is the sum of the many slowly decaying contributions of alternate signs, corresponding to the successive regions of positive and negative values of $\cos(\omega_I t)$.

- ¹ Adv. Inorg. Chem. Vol. **57**, edited by R. van Eldik and I. Bertini (2005).
- ² R. Kimmich and E. Anzardo, Prog. Nucl. Magn. Reson. Spectrosc. **44**, 257 (2004).
- ³ S. Wagner, T. R. J. Dinesen, T. Rayner, and R. G. Bryant, J. Magn. Reson. **140**, 172 (1999).
- ⁴ I. Bertini, C. Luchinat, and G. Parigi, *Solution NMR of Paramagnetic Molecules* (Elsevier, Amsterdam, 2001).
- ⁵ A. Carrington and A. D. McLachlan, *Introduction to Magnetic Resonance* (Harper, New York, 1967).
- ⁶ A. Messiah, *Quantum Mechanics* (North Holland, Amsterdam, 1961).
- ⁷ A. Redfield, Adv. Magn. Reson. **1**, 1 (1965).
- ⁸ I. Solomon, Phys. Rev. **99**, 559 (1955).
- ⁹ I. Solomon and N. Bloembergen, J. Chem. Phys. **25**, 261 (1956).
- ¹⁰ N. Bloembergen, J. Chem. Phys. **27**, 572 (1957).

- ¹¹ N. Bloembergen and L. O. Morgan, J. Chem. Phys. **34**, 842 (1961).
- ¹² P. Caravan, J. J. Ellison, T. J. McMurtry, and R. B. Lauffer, Chem. Rev. (Washington, D.C.) **99**, 2293 (1999).
- ¹³ S. Aime, M. Botta, M. Fasano, and E. Terreno, Chem. Soc. Rev. **27**, 19 (1998).
- ¹⁴ *Contrast Agents I: Magnetic Resonance Imaging* edited by W. Krause (Springer, Berlin, 2002).
- ¹⁵ *The Chemistry of Contrast Agents in Medical Magnetic Resonance Imaging* edited by E. Toth and A. E. Merbach (Wiley, Chichester, 2001).
- ¹⁶ N. Bloembergen, E. M. Purcell, and R. V. Pound, Phys. Rev. **73**, 679 (1948).
- ¹⁷ A. Abragam, *The Principles of Nuclear Magnetism* (Oxford University Press, Oxford, 1961).
- ¹⁸ J. Kowalewski and L. Mäler, *Nuclear Spin Relaxation in Liquids* (Taylor and Francis, New York, 2006).
- ¹⁹ D. Kruk, *Theory of Evolution and Relaxation in Multi-Spin Systems* (Arima, Bury St. Edmunds, 2007).
- ²⁰ S. Rast, P. H. Fries, and E. Belorizky, J. Chem. Phys. **113**, 8724 (2000).
- ²¹ P. H. Fries and E. Belorizky, J. Chem. Phys. **126**, 204503 (2007).
- ²² R. E. Connick and D. Fiat, J. Chem. Phys. **44**, 4103 (1966).
- ²³ J. Reuben, G. H. Reed, and M. Cohn, J. Chem. Phys. **52**, 1617 (1970).
- ²⁴ M. Gueron, J. Magn. Reson. (1969-1992) **19**, 58 (1975).
- ²⁵ N. Benetis, J. Kowalewski, L. Nordenskiöld, H. Wennerström, and P.-O. Westlund, Mol. Phys. **48**, 329 (1983).
- ²⁶ J. Kowalewski, D. Kruk, and G. Parigi, Adv. Inorg. Chem. **57**, 41 (2005).
- ²⁷ M. M. Mäkinen, L. C. Kuo, M. B. Yim, G. B. Wells, J. M. Fukuyama, and J. E. Kim, J. Am. Chem. Soc. **107**, 5245 (1985).
- ²⁸ A. Hudson and G. R. Luckhurst, Mol. Phys. **16**, 395 (1969).
- ²⁹ M. Rubinstein, A. Baram, and Z. Luz, Mol. Phys. **20**, 67 (1971).
- ³⁰ P.-O. Westlund, Mol. Phys. **85**, 1165 (1995).
- ³¹ E. Strandberg and P.-O. Westlund, J. Magn. Reson., Ser. A **122**, 179 (1996).
- ³² I. Bertini, O. Galas, C. Luchinat, and G. Parigi, J. Magn. Reson., Ser. A **113**, 151 (1995).
- ³³ R. R. Sharp, J. Chem. Phys. **93**, 6921 (1990).
- ³⁴ R. Sharp, L. Lohr, and J. Miller, Prog. Nucl. Magn. Reson. Spectrosc. **38**, 115 (2001).
- ³⁵ P.-O. Westlund, J. Chem. Phys. **108**, 4945 (1998).
- ³⁶ I. Bertini, J. Kowalewski, C. Luchinat, T. Nilsson, and G. Parigi, J. Chem. Phys. **111**, 5795 (1999).
- ³⁷ D. Kruk, T. Nilsson, and J. Kowalewski, Phys. Chem. Chem. Phys. **3**, 4907 (2001).
- ³⁸ T. Larsson, P.-O. Westlund, J. Kowalewski, and S. H. Koenig, J. Chem. Phys. **101**, 1116 (1994).
- ³⁹ S. Rast, A. Borel, L. Helm, E. Belorizky, P. H. Fries, and A. E. Merbach, J. Am. Chem. Soc. **123**, 2637 (2001).
- ⁴⁰ M. Odelius, C. Ribbing, and J. Kowalewski, J. Chem. Phys. **103**, 1800 (1995).
- ⁴¹ M. Odelius, C. Ribbing, and J. Kowalewski, J. Chem. Phys. **104**, 3181 (1996).
- ⁴² R. Sharp and L. Lohr, J. Chem. Phys. **115**, 5005 (2001).
- ⁴³ R. Sharp, J. Magn. Reson. **154**, 269 (2002).
- ⁴⁴ T. Nilsson and J. Kowalewski, J. Magn. Reson. **146**, 345 (2000).
- ⁴⁵ K. Åman and P.-O. Westlund, Mol. Phys. **102**, 1085 (2004).
- ⁴⁶ K. Åman and P.-O. Westlund, Phys. Chem. Chem. Phys. **9**, 691 (2007).
- ⁴⁷ S. Rast, P. H. Fries, E. Belorizky, A. Borel, L. Helm, and A. E. Merbach,

- J. Chem. Phys. **115**, 7554 (2001).
- ⁴⁸E. Belorizky and P. H. Fries, Phys. Chem. Chem. Phys. **6**, 2341 (2004).
- ⁴⁹P. H. Fries and E. Belorizky, J. Chem. Phys. **123**, 124510 (2005).
- ⁵⁰R. R. Sharp, J. Magn. Reson. (1969-1992) **100**, 491 (1992).
- ⁵¹R. R. Sharp, J. Chem. Phys. **98**, 2507 (1993).
- ⁵²R. R. Sharp, J. Chem. Phys. **98**, 6092 (1993).
- ⁵³S. M. Abernathy and R. R. Sharp, J. Chem. Phys. **106**, 9032 (1997).
- ⁵⁴N. Schaeffe and R. Sharp, J. Chem. Phys. **121**, 5387 (2004).
- ⁵⁵N. Schaeffe and R. Sharp, J. Magn. Reson. **176**, 160 (2005).
- ⁵⁶E. N. Ivanov, Zh. Eksp. Teor. Fiz. **45**, 1509 (1963); [Sov. Phys. JETP **18**, 1041 (1964)].
- ⁵⁷A. Abragam and B. Bleaney, *Electron Paramagnetic Resonance of Transition Ions* (Clarendon, Oxford, 1970).
- ⁵⁸D. Kruk and J. Kowalewski, Mol. Phys. **101**, 2861 (2003).
- ⁵⁹See EPAPS Document No. E-JCPSA6-128-028891 for additional figures. This document can be reached through a direct link in the online article's HTML reference section or via the EPAPS homepage (<http://www.aip.org/pubservs/epaps.html>).
- ⁶⁰J. Kowalewski, C. Luchinat, T. Nilsson, and G. Parigi, J. Phys. Chem. A **106**, 7376 (2002).
- ⁶¹D. Kruk and J. Kowalewski, J. Magn. Reson. **162**, 229 (2003).
- ⁶²D. Kruk and J. Kowalewski, JBIC, J. Biol. Inorg. Chem. **8**, 512 (2003).
- ⁶³P.-O. Westlund, H. Wennerström, L. Nordenskiöld, J. Kowalewski, and N. Benetis, J. Magn. Reson. (1969-1992) **59**, 91 (1984).
- ⁶⁴N. Benetis, J. Kowalewski, L. Nordenskiöld, H. Wennerström, and P.-O. Westlund, Mol. Phys. **50**, 515 (1983).
- ⁶⁵N. Benetis and J. Kowalewski, J. Magn. Reson. (1969-1992) **65**, 13 (1985).